IMPROVING COMBINED TACTILE-KINESTHETIC HAPTIC FEEDBACK THROUGH HAPTIC SHADING ALGORITHMS AND MECHANICAL DESIGN CONSTRAINTS

by

Andrew John Doxon

A dissertation submitted to the faculty of
The University of Utah
in partial fulfillment of the requirements for the degree of

Doctor of Philosophy

Department of Mechanical Engineering

The University of Utah

May 2014

The University of Utah Graduate School

STATEMENT OF DISSERTATION APPROVAL

The following faculty members served as the supervisory committee chair and members for the dissertation of Andrew John Doxon. Dates at right indicate the members' approval of the dissertation.

William Provancher, Chair	12-10-2013 Date Approved
Jake Abbot, Member	12-3-2013 Date Approved
Andrew Merryweather, Member	12-3-2013 Date Approved
David Johnson, Member	12-3-2013 Date Approved
Hong Tan, Member	12-5-2013 Date Approved

The dissertation has also been approved by Tim Ameel

Chair of the Department/School/College of Mechanical Engineering

and by David B. Kieda, Dean of The Graduate School.

ABSTRACT

Virtual environments provide a consistent and relatively inexpensive method of training individuals. They often include haptic feedback in the form of forces applied to a manipulandum or thimble to provide a more immersive and educational experience. However, the limited haptic feedback provided in these systems tends to be restrictive and frustrating to use. Providing tactile feedback in addition to this kinesthetic feedback can enhance the user's ability to manipulate and interact with virtual objects while providing a greater level of immersion. This dissertation advances the state-of-the-art by providing a better understanding of tactile feedback and advancing combined tactile-kinesthetic systems. The tactile feedback described within this dissertation is provided by a finger-mounted device called the contact location display (CLD). Rather than displaying the entire contact surface, the device displays (feeds back) information only about the center of contact between the user’s finger and a virtual surface.

In prior work, the CLD used specialized two-dimensional environments to provide smooth tactile feedback. Using polygonal environments would greatly enhance the device's usefulness. However, the surface discontinuities created by the facets on these models are rendered through the CLD, regardless of traditional force shading algorithms. To address this issue, a haptic shading algorithm was developed to provide smooth tactile and kinesthetic interaction with general polygonal models. Two experiments were used to evaluate the shading algorithm.

To better understand the design requirements of tactile devices, three separate experiments were run to evaluate the perception thresholds for cue localization, backlash, and system delay. These experiments establish quantitative design criteria for tactile devices. These results can serve as the maximum (i.e., most demanding) device specifications for tactile-kinesthetic haptic systems where the user experiences tactile feedback as a function of his/her limb motions.

Lastly, a revision of the CLD was constructed and evaluated. By taking the newly evaluated design criteria into account, the CLD device became smaller and lighter weight, while providing a full two degree-of-freedom workspace that covers the bottom hemisphere of the finger. Two simple manipulation experiments were used to evaluate the new CLD device.

TABLE OF CONTENTS

ACKNOWLEDGEMENTS

It has been a long journey to my PhD dissertation. I would first like to thank all those around me who I learn from on a daily basis. Without you I would not have grown into the person I am today. While those around me may change from year to year, I will continue to develop and learn from you for the rest of my life. To you I give thanks from the bottom of my heart.

I want to thank my parents, who have dedicated over a third of their lives helping me succeed. They support me in my decisions and give me sound advice when I ask for it. I am very lucky to have them. I would especially like to thank my father who has listened to my ramblings about my research even when he may not understand it all. He has forced me to explain things in simpler terms and in doing so improved my work.

I would like to thank the many teachers I have had over the years. Not all of you were my favorite but I learned from every one of you. You enabled me to continue feeding my natural curiosity about the world and everything in it. I especially want to thank Dr. William Provancher, my advisor, with whom I have spent the last 5 years, for admitting me into his research group and allowing me to work on a number of interesting projects. He has taught me so many things in the time I have known him, and for that I am beyond grateful. I would also like to thank Hong Tan and David Johnson for vetting my ideas and working with me on the studies presented in this dissertation. I also want to thank my lab

partner Muhammad Yazdian for always letting me bounce research ideas off him and refine my experiments.

Finally, I would like to thank the National Science Foundation for their grant money under awards IIS-0904456 and IIS-0746914 that made my stay at the University of Utah and this research possible.

CHAPTER 1

INTRODUCTION

Training in virtual environments is becoming more and more common as the demand for highly trained professionals increases, such as in medical practice. Virtual environments provide a consistent and relatively inexpensive method of training individuals. In medical practice, this translates to significantly lower costs and also provides doctors additional training before their first human patient. High quality graphics and powerful physics simulations are the norm in these systems. These virtual environments often include haptic feedback in the form of forces applied to a manipulandum or thimble to provide a more immersive and educational experience. However, the limited haptic feedback provided in these systems tends to be restrictive and frustrating to use. By only providing kinesthetic (force) feedback, these systems limit the user's ability to dexterously interact with and manipulate their environment [1]. Providing tactile feedback in addition to this kinesthetic feedback can enhance the user's ability to manipulate and interact with virtual objects while providing a greater level of immersion. Studies have shown that providing tactile feedback in concert with kinesthetic information can dramatically improve one's ability to dexterously interact with and explore virtual environments [2], [3], [4].

The research presented in this dissertation helps to refine combined tactile-kinesthetic feedback through a finger-mounted device called the contact location display (CLD).

Rather than displaying the entire contact surface, the device displays only the center of contact between the user's finger and a virtual surface. Figure 1.1 presents the concept of contact location feedback. While other devices provide more complex colocated tactile and kinesthetic feedback cues, contact location feedback was chosen as a simple, intuitive, and computationally efficient method of providing tactile feedback. Although the contact location display does not provide the contact profile directly, it is still capable of conveying curvature and other important surface properties [5]. The simple mechanical requirements for rendering contact location allow a smaller, more compact device design. This compactness allows the device to be integrated with many commercially available force feedback devices.

This document presents the results of several studies that help refine the contact location display and haptic interfaces in general. The first of these studies presents algorithms that allow many tactile devices, such as those found in [3], [6], and [7] which use specialized environments, to take advantage of generalized polygonal environments. Polygonal modeling allows complex environments to be created easily and quickly, while specialized environments often take time to create even simple shapes. By providing algorithms that allow researchers to use their devices more easily in polygonal environments, we help them perform more and varied experiments while also making it

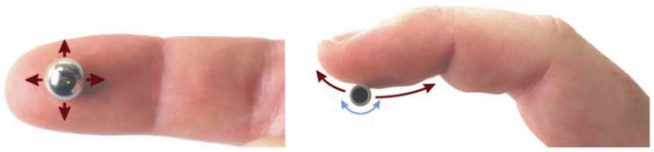

Figure. 1.1 Concept for contact location feedback. The two-dimensional (left) or one-dimensional (right) center of contact is represented with a single tactile element. The prior contact location display (CLD) was only capable of displaying one-dimensional contacts along the length of the finger. However, a two degree-of-freedom CLD design has now been designed and is presented herein.

easier to combine their device with commercially available devices. The second study focused on providing design criteria to provide a better understanding of the limits of human perception. These results provide a framework for future tactile device designs as well as potentially loosening the design requirements of current devices, allowing them to be smaller and less expensive without compromising their performance. The last study revises the CLD device to improve interactions in three-dimensional (3D) environments and enable future research into multifinger manipulation. It acts as a demonstration of the prior studies' findings.

Our first study helped improve tactile displays by presenting algorithms to provide smooth interaction with polygonal models. Many tactile displays require specialized environments to function. In contrast, commercially available kinesthetic displays commonly use general polygonal models to generate haptic interaction. Using two- and three-dimensional (2D and 3D) polygonal geometric models would significantly expand the device's usefulness. However, when interacting with polygonal approximations to smooth surfaces, the CLD, and other tactile displays, transmits the surface discontinuities to the user. This gives the impression that the surface is rough or textured rather than smooth, and is distracting to the user even when interacting with high-count polygonal models. The use of shading algorithms not only reduces the effects of surface discontinuities but can also lead to a significant reduction in model size while still retaining a surface that feels smooth. Traditional shading algorithms do not compensate for discontinuities in the model surface and thus cannot be used with tactile displays like the CLD. To address this issue, we developed new haptic shading algorithms to provide smooth tactile and kinesthetic feedback. The presented shading algorithms create a

smooth continuous surface by interpolating surface geometry and vertex normals which is then used to compute tactile and kinesthetic feedback. Two experiments were run to evaluate the shading algorithms. The first experiment measured the perception thresholds for rendering faceted objects as smooth. It was found that the addition of contact location feedback in the absence of tactile shading significantly increased user sensitivity to edges. The shading algorithm was shown to reduce the number of needed facets to create a tactilely smooth surface. The second experiment evaluated the effects of providing contact location feedback during exploration and shape recognition within a 3D environment. While the second study provided validation for our shading algorithm, the results of the study showed no significant effect of the CLD and underscored the need for improvements in the device design before it could effectively be used in 3D environments.

Our initial attempts to expand the tactor motion of the device to two degrees-of-freedom (DOF) resulted in a reduced workspace and high tactor backlash, limiting the effectiveness of the device [8]. These problems were brought about by attempting to meet specifications that far exceeded human sensing thresholds while attempting to maintain a small device profile. By relaxing design requirements and designing more closely to match the limits of human perception, devices can become smaller, less expensive, and more useful. Thus, our second study performed three separate experiments to evaluate the perception thresholds for cue localization, backlash, and system delay. The results of these experiments effectively establish quantitative design criteria for tactile devices. The first of these experiments evaluated the ability of humans to repeatedly localize tactile cues across the fingerpad. These results state the maximum positioning error that the

device should achieve after large or sequential motions. The second experiment measured the minimum detectable backlash of a tactor on the fingerpad during active exploration. These results directly stipulate the maximum backlash a device should contain at its tactile element. The third experiment determined the minimum detectable system delay between user action and device motion. These results can serve as the maximum (i.e., most demanding) device specifications for tactile-kinesthetic haptic systems where the user experiences tactile feedback as a function of their limb motions.

Lastly, a revision of the CLD for use in 3D environments was constructed and evaluated. By taking the newly evaluated design criteria into account, the CLD device became smaller and lighter weight, while providing a full 2-DOF workspace that covers the bottom hemisphere of the finger. The new CLD design is particularly well suited for multifinger manipulation due to its small size and the large amount of finger dexterity retained during use, while previous revisions were not well suited for a multifinger setup due to size or mounting restrictions. Our third study consisted of two simple manipulation experiments, used in evaluation of the new CLD device. A postexperiment survey was used to evaluate participant perceptions of performance and device effects. The first experiment evaluated a participant's ability to successfully pick up a series of spheres with varying levels of friction. The results showed a significant improvement in the number of tries to successfully pick up the sphere when contact location feedback is provided. Task completion time did not change with respect to the feedback provided. These results agreed with the postexperiment survey. The second experiment evaluated a participant's ability to successfully identify the position and orientation of a flat on a cylindrical object and reorient that object with respect to a fixed reference orientation.

Providing contact location feedback showed no statistical effect on alignment error. However, it did show a negative effect on completion time by an average of 7 seconds. The postexperiment survey indicated this extra time might have been due to an oversaturation of haptic information, forcing the participant to move more slowly. Thus, the CLD should ideally be used in situations where the extra surface information it provides is needed for the task.

1.1 Contributions

Three main contributions were made through this research: development of tactile shading algorithms, evaluation of perceptual thresholds, and revisions to the CLD device.

1. Development of two haptic shading algorithms for use in 2D and 3D, respectively.

   Haptic shading algorithms for general polygonal models to provide smooth tactile and kinesthetic feedback were developed. These algorithms create a smooth continuous surface used to compute tactile and kinesthetic feedback by interpolating surface geometry and vertex normals. The algorithms are computationally efficient, only requiring local surface geometry, allowing interactions with complex environments and arbitrary finger models without a performance decrease. These shading algorithms expand the usefulness of tactile devices with consumer products by allowing them to be used outside of specially constructed environments.

2. Evaluation of perceptual thresholds.

   Perception thresholds were evaluated to expand our understanding of tactile devices and haptic feedback. Perception thresholds for rendering

faceted objects as smooth were determined. These thresholds identify the minimum angle between adjacent facets of a polygonal model that must be maintained for the model to be perceived as "smooth" under different rendering conditions. Quantitative device design criteria were created through measuring the perception thresholds for cue localization, backlash, and system delay. These design criteria can be applied to nearly any tactile device where tactile feedback is directly related to user finger motions.

3. Revisions of the CLD device.

   The original 1-DOF CLD device was improved by redesigning and fabricating a lighter actuator box with a better mounting bracket. The device thimble was also redesigned to eliminate feedback instabilities when contacting virtual objects with the front or top of the finger. A revised 2-DOF device was developed and presented in Chapter 4. This device improves upon previous CLD devices by being smaller, lighter weight, and containing a larger workspace. The device allows exploration of the effects of contact location in multifinger manipulation tasks as well as providing better interactions with virtual objects, allowing users to detect relative object position and motion more clearly.

1.2 Chapter Overview

The following section gives a brief overview of each chapter.

Chapter 2 defines two haptic shading algorithms that allow tactile displays to smoothly interact with 2D and 3D general polygonal models, respectively. Two experiments were run to evaluate these haptic shading algorithms. The first measures

perception thresholds for rendering faceted objects as smooth objects. The second experiment explored the CLD device's ability to facilitate exploration and shape recognition within a 3D environment.

Chapter 3 establishes quantitative design criteria for tactile devices. Specifically, this chapter outlines the perceivable thresholds for cue localization, backlash, and system delay through three separate experiments. The obtained results can serve as the maximum (i.e., most demanding) device specifications for tactile-kinesthetic haptic devices where the user is experiencing tactile feedback as a function of their hand motions.

Chapter 4 describes the design and characterization of a more advanced and compact CLD device. The new device is smaller, lighter weight, and provides a full 2-DOF workspace that covers the bottom hemisphere of the finger. Two simple manipulation experiments are used in evaluation of the device. The first experiment evaluated each participant's ability to successfully pick up a series of spheres with varying levels of friction. The second experiment evaluated each participant's ability to successfully identify the position and orientation of a flat on a cylindrical object, then reorient that object with respect to a fixed reference frame.

Chapter 5 provides a conclusion to this dissertation and discusses the next steps in continuing this research.

1.3 References

[1] A. Frisoli, M. Bergamasco, S. L. Wu, and E. Ruffaldi. Evaluation of Multipoint Contact Interfaces in Haptic Perception of Shapes. In Multi-point interaction with real and Virtual Objects, Springer Berlin Heidelberg, pp. 177-188, 2005.

[2] S. Lederman and R. Klatzky. Sensing and displaying spatially distributed fingertip forces in haptic interfaces for teleoperator and virtual environment systems. Presence: Teleoperators and Virtual Environments, vol. 8, no. 1, pp. 86-103, Feb. 1999.

[3] A. Frisoli, M. Solazzi, F. Salsedo, and M. Bergamasco. A fingertip haptic display for improving curvature discrimination. Presence: Teleoperators and Virtual Environments, vol. 17, no. 6, pp. 550-561, Oct. 2008.

[4] R. Fearing. Tactile Sensing, Perception and Shape Interpretation. PhD thesis, Electrical Engineering: Stanford University, Stanford, CA, USA, 1988.

[5] W. R. Provancher, M. R. Cutkosky, K. J. Kuchenbecker, and G. Niemeyer (2005). Contact location display for haptic perception of curvature and object motion. International Journal of Robotics Research, vol 24(9), pp. 691–702, 2005.

[6] I. Sarakoglou, N. Garcia-Hernandez, N. Tsagarakis, and D. Caldwell. A high performance tactile feedback display and its integration in teleoperation. IEEE Transactions on Haptics, vol. 5, no. 3. pp. 252-263, 2012.

[7] D. Prattichizzo, C. Pacchierotti, and G. Rosati. Cutaneous force feedback as a sensory subtraction technique in haptics. IEEE Transactions on Haptics, vol. 5, no. 4, pp. 289-300, 2012.

[8] S. Yazdian, A. J. Doxon, D. E. Johnson, H. Z. Tan, and W. R. Provancher. 2-DOF contact location display for manipulating virtual objects. In 2013 World Haptics Conference (WHC), pp. 443-448, 2013.

CHAPTER 2

FORCE AND CONTACT LOCATION SHADING METHODS FOR USE WITHIN TWO- AND THREE-DIMENSIONAL POLYGONAL ENVIRONMENTS

The following journal publication consists of material originally presented in my Master of Science Thesis. For a more complete representation of this work, please see my thesis presented under the title "Force and Contact Location Shading Methods for Use Within Two- and Three-Dimensional Polygonal Environments," presented at the University of Utah in 2010. As my dissertation represents my cumulative work in the area of haptics at the University of Utah, this publication has been included for completeness and as one of my contributions toward improving tactile-kinesthetic haptic feedback.

"Force and Contact Location Shading Methods for use Within Two- and Three-Dimensional Polygonal Environments,"

A. J. Doxon, D. E. Johnson, H. Z. Tan, and W. R. Provancher.

Abstract—Current state-of-the-art haptic interfaces only provide kinesthetic (force) feedback, yet studies have shown that providing tactile feedback in concert with kinesthetic information can dramatically improve one's ability to dexterously interact with and explore virtual environments. In this research, tactile feedback was provided by a device, called a contact location display (CLD), which is capable of rendering the center of contact to a user.

The chief goal of the present work was to develop algorithms that allow the CLD to be used with polygonal geometric models, and to do this without the resulting contact location feedback being overwhelmed by the perception of polygonal edges and vertices. Two haptic shading algorithms were developed to address this issue and successfully extend the use of the CLD to 2D and 3D polygonal environments.

Two experiments were run to evaluate these haptic shading algorithms. The first measured perception thresholds for rendering faceted objects as smooth objects. It was found that the addition of contact location feedback significantly increased user sensitivity to edges and that the use of shading algorithms was able to significantly reduce the number of polygons needed for objects to feel smooth.

1 Introduction

HUMAN-computer interfaces that involve the sense of touch, or haptic interfaces, are becoming more and more prevalent throughout the world. Despite this, these devices are still often restrictive and frustrating to use, which keeps them far from their full potential as intuitive human-computer interfaces.

Most current haptic interfaces provide a purely kinesthetic interaction within virtual environments. This results in a significant loss of dexterity, as reported by Frisoli, Bergamasco, Wu, and Ruffaldi (2005). If implemented well, providing tactile feedback in combination with kinesthetic information should dramatically improve one's ability to dexterously interact and explore virtual environments, to potentially provide an improvement similar to when people remove a pair of gloves.

One such system that provides both tactile and kinesthetic feedback is the contact location display (CLD) developed by Provancher, Cutkosky, Kuchenbecker, and Niemeyer (2005) attached to a PHANToM. In addition to forces, this device displays the contact location between a virtual finger and a surface to the user. Figure 1 shows the concept for a contact location display.

Figure 1. Concept for contact location feedback. The (left) two-dimensional or (right) one-dimensional center of contact is represented with a single tactile element.

Previously, the CLD device was utilized only with specialized 2D models. Use of 3D polygonal geometric models, as is common in both haptics and computer graphics (Ruspini & Khatib, 2001), with the CLD device would significantly expand the device's usefulness by allowing combined tactile and kinesthetic feedback in these common virtual environments without requiring model conversion or preprocessing.

However, when interacting with polygonal approximations to smooth surfaces, the CLD transmits the surface discontinuities to the user. This gives the impression that the surface is meant to be rough or textured rather than smooth and it is distracting to the user even when interacting with high-count polygonal models. The use of shading algorithms can not only reduce the effects of surface discontinuities but also lead to a significant reduction in model size while still retaining a surface that feels smooth.

Force shading, as developed by Morganbesser and Srinivasan (1996), smoothes the faceted models by interpolating the surface normal between vertices. Discontinuities in the form of proprioceptive (position) cues remain present. Humans, in general, find it difficult to detect these proprioceptive cues so the smooth force interactions override the weaker proprioceptive signals and a smooth object is perceived. However, contact location is dependent on the object's surface and the virtual

- *A.J. Doxon is with the department of Mechanical Engineering, College of Engineering, University of Utah, Salt Lake City, UT 84112. Email: adoxon@gmail.com*
- *D.E. Johnson is with the School of Computing, College of Engineering, University of Utah, Salt Lake City, UT 84112. Email: dejohnso@cs.utah.edu*
- *H.Z. Tanis with the School of Electrical and Computer Engineering, College of Engineering, Purdue University, West Lafayette, IN 47907. Email: hongtan@purdue.edu*
- *W.R. Provancher is with the department of Mechanical Engineering, College of Engineering, University of Utah, Salt Lake City, UT 84112. Email: wil@mech.utah.edu*

finger, which are not altered by Morganbesser and Srinivasan's force shading. The state-of-the-art is therefore incapable of eliminating the discontinuities in the tactile feedback for the CLD device (and other tactile displays).

This article presents two related haptic shading algorithms to provide smooth tactile and kinesthetic feedback for use within general 2D and 3D polygonal environments. These algorithms are designed to provide only a single point of contact, matching the display capabilities of the CLD device, and function on both convex and concave surfaces. The 2D shading algorithm was developed, implemented, and tested with human subjects to determine the feasibility of our approach and to obtain perceptual thresholds for rendering smooth objects. A more advanced 3D algorithm was then developed and tested using the results from the first experiment. The algorithms each derive locally smooth feedback from the original polygonal model. Some advantages of the algorithm include improved kinesthetic display over just using force shading and smoothed contact location feedback in the presence of polygonal artifacts. Furthermore, our approach is computationally efficient, making smoothed interactions feasible with complex environments and arbitrary finger models.

The following section provides a brief background concerning the literature most relevant to this research. This is followed by a description of the CLD device. The 3D algorithm is then presented in detail, with details of the 2D algorithm presented in the appendix. We then present two human subject experiments. The first experiment establishes the necessary polygonal mesh parameters for shaded polygon objects to feel perceptibly smooth. The second experiment is an object identification task, which provides a validation of the developed 3D algorithm and provides insights and inspiration for future work to further improve the efficacy of contact location feedback.

2 BACKGROUND

2.1 Combined Tactile and Kinesthetic Feedback

A number of studies have been conducted with combined tactile and kinesthetic feedback. Salada et al. conducted several studies that investigated the use of slip or sliding feedback in combination with kinesthetic motions (Salada, Colgate, Vishton, & Frankel, 2005). Salada was able to show that the addition of slip feedback allowed users to track small moving features better. The saliency of friction is also increased with skin stretch and slip feedback (Provancher & Sylvester 2009). Since then, others have also developed slip displays and integrated them with kinesthetic force feedback devices (Fritschi, Ernst, & Buss, 2006; Webster, Murphy, Verner, & Okamura, 2005). These devices tend to be large and cumbersome since a smaller contact area on the finger relates to weaker sliding cues. Fritschi et al. (2006) found that users judged interactions with slip feedback as more "real." Additionally, Fritschi et al. also investigated providing tactile slip feedback with a tactile pin array in combination with kinesthetic feedback (Fritschi et al., 2006). Again, Fritschi et al. found that providing slip feedback from a pin array increased the "realism" of the models. Like slip displays, pin arrays tend to be large and cumbersome. However, the true benefit of pin arrays is the variety of interactions possible with the device. Each pin can be individually controlled to create the sensation of textures across virtual surfaces.

Other interesting approaches to tactile-kinesthetic display include research on displaying the local object surface tangent (Dostmohamed & Hayward, 2005), (Frisoli, Solazzi, Salsedo, & Bergamasco, 2008). Dostmohamed and Hayward present a device that utilizes a gimbaled plate to represent the local surface tangent plane of virtual objects. The motion of the gimbaled plate is coordinated with the user's kinesthetic motions to display curved objects (Dostmohamed & Hayward, 2005). Dostmohamed and Hayward were able to demonstrate that by providing only an objects tangent plane through a gimbaled plate, participants were capable of curvature discrimination on par with real life exploration of large objects. As a relatively sophisticated adaptation of the this work, Frisoli et al. present a miniaturized finger-based tilting plate tactile display that can be attached to a kinesthetic display (Frisoli et al., 2008). Their results indicate a significantly improved performance in curvature discrimination when kinesthetic cues are also given.

Finally, Provancher's prior studies have shown the potential of contact location feedback for enhancing object curvature and motion cues (Provancher et al., 2005). The contact location display (CLD) has been shown to increase awareness of curvature change and edges which enables better contour following (Kuchenbecker, Provancher, Niemeyer, & Cutkosky, 2004).

2.2 Haptic Shading Algorithms

Haptic shading algorithms are developed to make polygonal representations of smooth objects feel smooth. Without haptic shading algorithms polygonal models of smooth objects feel rough and textured, which detracts from the desired haptic experience. Most shading algorithms either directly modify the interaction with the polygonal model or alter the position of a virtual proxy, a copy of the virtual finger left on the model's surface to which forces are rendered.

The most widely used haptic shading algorithm was developed by Morganbesser and Srinivasan (1996). This algorithm linearly interpolates surface normals on the environment models to guarantee a continuously smooth gradient. The graphics community uses a similar technique called Phong shading to create smooth normals for evaluating illumination across polygonal surfaces (Phong, 1973). Morganbesser and Srinivasan's algorithm was designed to reduce the "popping" effect felt in rendered normal forces when the haptic interaction point passes over a vertex or edge of a polygonal object. As with Phong shading, Morganbesser and Srinivasan found that their force shading algorithm helped give the sensation of a smoother object.

Ruspini et al. also incorporated a force shading model which interpolates the normals of the surface (Ruspini, Kolarov, & Khatib, 1997). In this case, a two-pass technique was utilized to modify the position of the virtual proxy. The first stage computes the closest point on the plane defined by the interpolated normal and the current proxy position. The second stage computes proxy forces as usual but uses the previously found closest point as the user-controlled point. This method reduces instability issues generated by using the original Morganbesser and Srinivasan algorithm when the haptic interaction point is in contact with multiple intersecting shaded surfaces.

An alternative to shading polygonal surfaces is to work directly with NURBS (non-uniform rational B-spline surfaces) models. Rather than approximating a surface, NURBS models use piecewise rational surfaces with controllable smoothness to precisely represent shapes. Existing approaches for haptic rendering of these models exploit tracking of a local contact point on the model (Thompson & Cohen, 1999; Johnson & Cohen, 1999) and between two models. However, creation of detailed NURBS models is still a complex task, and conversion from arbitrary models with complex topologies even more so. This paper provides a direct means of haptic interaction with polygonal mesh surface models while retaining some of the tracking and surface smoothness properties algorithms for NURBS models.

Other model representations, like the voxel approach presented by McNeely, Puterbaugh, and Troy (1999), include haptic shading through the summation of each voxel in the modeled environment. In this way small motions create small changes across multiple voxels thus creating the effect of a smooth interaction. However, methods like these provide only forces and cannot provide a contact location to be rendered with the CLD.

3 Experimental Apparatus

The concept for contact location feedback is presented in Figure 1, where only the center of contact is rendered. The hardware utilized in the following experiments consists of a SensAble PHANToM Premium 1.5, and a one degree-of-freedom (1-DOF) contact location display (CLD) device which displays contacts along the finger (see Figures 2 and 3). The PHANToM is used to render contact forces. The contact location display is used to render the current contact position on the finger. The device utilizes a 1 cm diameter delrin roller as a tactile contact element. The position of the roller on the finger is actuated

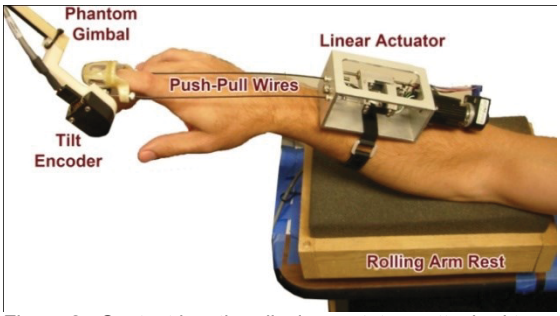

Figure 2. Contact location display prototype attached to a PHANToM robot arm. The user's elbow is supported by a rolling armrest.

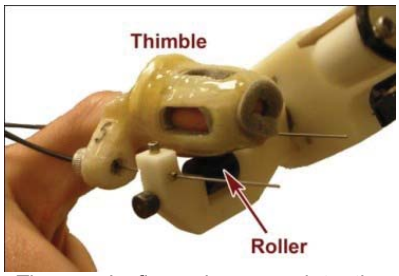

Figure 3. The user's finger is secured to the contact location display via an open-bottom thimble.

via sheathed push-pull wires attached to a linear actuator mounted on the user's forearm. The display's contact roller is directly attached to the PHANToM via a 1-DOF gimbal with sensed tilt angle. The roller is suspended beneath the fingerpad by the drive wires so that it does not touch the user's finger until contact is made with a virtual object. Contact forces, provided by the PHANToM, push the roller into contact with the user's fingerpad. An open-bottom thimble is used to attach the device securely to a user's finger and also provides a mounting point to anchor the sheaths of the spring steel drive wires. Several interchangeable thimbles, which together accommodate a wide range of finger sizes, were created using fused deposition modeling (FDM) rapid prototyping.

The linear actuator is located on the user's forearm to prevent any possible device vibrations from being transmitted to the user's fingertip receptors and to reduce the device inertia located at the fingertip. The linear actuator utilizes a Faulhaber 2342CR DC brushed motor and a 3.175 mm pitch leadscrew to provide approximately 2 cm of linear motion with approximately 0.8 μm of resolution and a bandwidth in excess of 5 Hz. A prototype of the device can be seen in Figure 2. A close-up view of the fingertip portion of the device is shown in Figure 3.

The device's motor is driven by an AMC 12A8 PWM amplifier that is controlled using a Sensoray 626 PCI control card. The device's PID controller was run at 1 kHz and was programmed in C++. The control program was executed under Windows XP using Windows multimedia timers. Further details about the design and control of this device may be found in Provancher et al. (2005).

4 Contact Location Rendering and Haptic Shading

4.1 Smooth vs. Faceted Surfaces

Many models in virtual environments are composed of faceted triangle meshes, even when the desired shape is smooth and continuous. In order to facilitate the use of tactile feedback during manipulation the original smooth shape must be recovered. Without smoothing, the edges of the triangle mesh dominate all other tactile information provided by the CLD.

The motion of the CLD device depends on the shape of the model used. The tactile motion of the CLD device traveling over a smooth curve in comparison to faceted surfaces is demonstrated in Figure 4. Note that the contact location smoothly changes while moving along a curved surface, whereas the contact location moves rapidly along the finger when crossing a vertex, and remains stationary while traversing a flat facet.

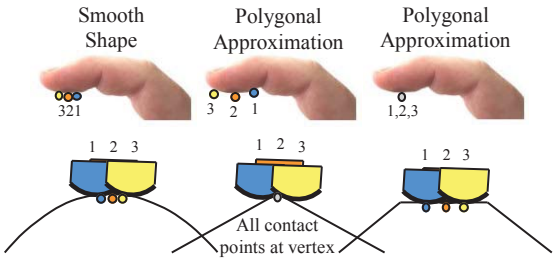

Figure 4. Contact location movement over a smooth round surface represented (left) with a curved surface model, (middle) with two facets, and (right) with three facets. The top shows a view of the fingerpad with a series of displayed contact locations, corresponding by color and number to the virtual finger positions below.

The following sections describe our algorithms to recover a smoothed version of a faceted model and to use this smoothed surface to render appropriate kinesthetic and tactile cues during contact.

4.2 Overview of Developed Algorithms

Both the 2D and 3D smoothing algorithms presented in this paper utilize Bézier curves/surfaces to generate smooth interactions. These curves/surfaces are temporarily generated from a control polygon produced from the underlying environment model around the region of contact. The resulting Bézier curve/surface is then used with the finger model to determine the proper contact location and force feedback parameters. This approach is a hybrid of prior work on rendering and shading triangular mesh models and work on rendering parametric models, such as splines, as it works directly with the given polygonal models yet locally generates a temporary parametric surface for smoothing.

In general, computing the contact location between two curves, the finger model and curved environment model, requires robust numerical methods that may run too slowly for haptic applications (Seong, Johnson, Elber, & Cohen, 2010). Instead, our algorithm computes a dynamically updated tangent line/plane at the point of contact. This reduces the computation needed to evaluate the interaction between a line/plane and the finger model. This interaction is rendered as a single point that is constrained to lie on the finger model's surface, which matches

the display capabilities of the CLD. Thus, the approach is not based purely on a point-model or model-model interaction, but instead lies somewhere in-between.

By ensuring the environment model is a fully connected and continuous manifold mesh we can guarantee the resulting curve/surface is continuous and smooth. Multiplicity, or multiple points/normals defined at the same coordinates, can be used to generate sharp corners on the rendered smooth surface when desired.

In brief, the algorithms perform the following steps:

1. First the model is broken into a local control polygon/mesh.
2. The contact location with the current tangent line/plane is computed to evaluate finger motion with respect to the surface.
3. Given the local control polygon/mesh and motion along the tangent, the motion along the smoothed surface is approximated and a new tangent line/plane is computed.
4. This approximation iterates until convergence with the true contact location is reached.
5. The final tangent after convergence is then used to compute the displacement of the CLD as well as the smoothed forces rendered by the PHANToM.

While the algorithm was developed to provide both smooth tactile and kinesthetic feedback it can also be used as a substitute for the methods presented by Morganbesser and Srinivasan (1996) for force shading.

Details of the 3D Haptic Shading Algorithm are presented below, while the 2D Algorithm that was used in our discrimination threshold study is included, for completeness, in the appendix.

4.3 Overview of the 3D Haptic Shading Algorithm

Each primitive triangle element of the polygonal model is used to generate the control mesh of a curved surface, in this case with a variant of Bézier triangles which provides contact continuity and smoothness. While it is possible to fit smooth surfaces to polygonal models, the process is difficult and time consuming (Cohen, Riesenfeld, & Elber, 2001; Daniels, Silva, Shepherd, & Cohen, 2008).

We adapted a technique from the computer graphics literature, PN (point normal) triangles (Vlachos, Peters, Boyd, & Mitchell, 2001), which produce control meshes for Bézier triangles and quadratic interpolation based solely on the original triangle vertices and their corresponding normal vectors. This allows PN triangles to perform local smoothing processes independently of the number of triangles in the mesh which is necessary for smoothing large models at haptic rates. Evaluation of PN triangles directly defines the tangent plane used in the haptic rendering algorithm. The Bézier triangle surface provides the point and the quadratically interpolated normals provide the normal.

The process followed by the 3D algorithm uses numerical methods to converge to the ideal contact point. Thus within each haptic rendering cycle (a minimum of 1000 Hz) this process is repeated until the ideal contact point is reached, that is, until the proxy's contact location is the point generated by the Bézier triangle surface. The user's movement is only captured once each haptic rendering cycle. To facilitate fast rendering times each triangle in the mesh also contains information on its three adjacent triangles.

Fully smoothed surfaces can lose important detail. The presented approach allows preservation of straight edges through the addition of multiple normals on a single vertex. These normals must be defined perpendicular to the straight edge or the PN triangle surface will become discontinuous, creating a hole in the surface. For curved edges, it is advised instead to add smaller triangles along the edge to more accurately define the feature.

4.4 PN Triangles

4.4.1 Defining the Control Mesh

PN triangles use barycentric coordinates, which are commonly used to define positions on triangles in terms of u, v, and w, as parametric coordinates. They are a system of homogenous coordinates based on the signed areas of the base triangle and the subtriangles formed by the target point.

The Bézier triangle's control mesh in PN triangles is defined by ten points. This creates a 3rd order surface in all three barycentric coordinates (u, v, and w). Third order surfaces were chosen because they are the minimum degree capable of rendering inflections in surface contours. The control mesh is computed from the base triangle's points (P_1,P_2,P_3) and their corresponding normals (N_1,N_2,N_3). For the specific method of computing all ten control points, the reader is referred to Vlachos et al.

(2001).

Each edge of the control mesh is determined only by the two points comprising that edge. Thus the edges of two adjacent PN triangles are contiguous. Figure 5 shows a shaded base triangle and its corresponding control mesh. The three outer-most triangles are created such that they share the base triangle's corners and normals. The center point, b_{111}, is defined as an extension of the six new middle points with respect to the original center of the base triangle.

The naming convention chosen in this paper is the same as that used by Vlachos et al. (2001).

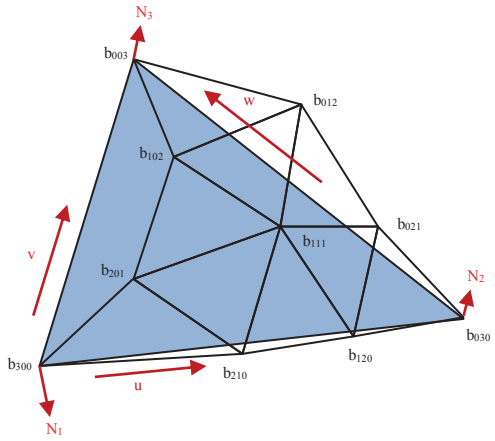

Figure 5. A control mesh generated for a particular base polygon. The mesh is defined completely by the three normals defined at each of the three vertices on the base polygon and their relationships. Arrow vectors show the directions of the barycentric coordinates u, v, and w used as parametric inputs.

The base indices on the mesh represent the position and weight of each corner of the base triangle on the individual point. Thus in Figure 5, the index of b_{012} indicates it is influenced proportionally by 0/3 of P_1, 1/3 of P_2, and 2/3 of P_3. The weights always sum to the order of the system being made.

The control mesh for the quadratically interpolated normals contains only six points and defines a second order system. The specific equations used by Vlachos et al. (2001) help guarantee that if there is an inflection in the surface it will also be represented in the normals. Since this control mesh is constructed of normal vectors, all its vectors must be normalized to 1 before being used. The second control mesh uses the same naming scheme as the first (e.g. n_{110}). Since it is second order the weights will only sum to 2.

4.4.2 *Computing the PN surface*

Given the control meshes and a set of barycentric coordinates a point and normal on the surface can be computed. Equations are provided by Vlachos et al. (2001) to directly compute a single point and normal on the PN triangle surface. Using these continuous surface points and normals we can guarantee that the resulting contact location will also be continuous. While a method for recursively computing the surface point and normal does exist for Bézier triangles (as the one used in the 2D algorithm) it is faster to compute the result directly in this case.

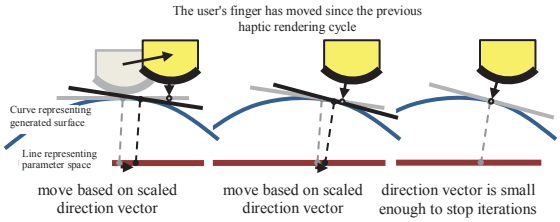

Figure 6. The tangent plane converges to the ideal contact point where the proxy contact point is the rendered surface point and is drawn chronologically from the left to the right. The previous iteration is shown in gray.

4.5 Implementing the 3D Haptic Shading Algorithm

This section provides detailed descriptions of each step taken in the algorithm. As the user moves, the shading algorithm computes a point and tangent plane on the smoothed surface.

Figure 6 demonstrates the basic iterative process performed by the shading algorithm for a typical 2D cross-section of a shaded surface. The user's finger is orthogonally projected onto the previous iteration's tangent plane (shown in grey) to compute a contact position. This contact position is used to compute the current tangent plane (shown in black). This is repeated until the tangent planes become nearly identical. The final tangent plane is then used to compute the haptic interaction.

4.5.1 *Computing the Current Proxy Contact Location*

In this step, the updated position of the user is orthogonally projected toward the tangent plane created in the previous iteration. The initial contact between the finger model and tangent plane defines a new contact position. A direction vector can then be created between the previous contact position to the current contact point. This direction vector represents a reasonable linear approximation of the motion along the base triangle needed to compute the barycentric coordinates that will result in a more accurate

surface rendering thus allowing the system to converge given a sufficiently small step size.

4.5.2 Computing the New Parameter Value

The direction vector found in the previous step is used to compute a new set of barycentric values by projecting it onto the plane of the base triangle. Figure 7 shows the travel direction vector, its projection, and the new surface point due to that projection.

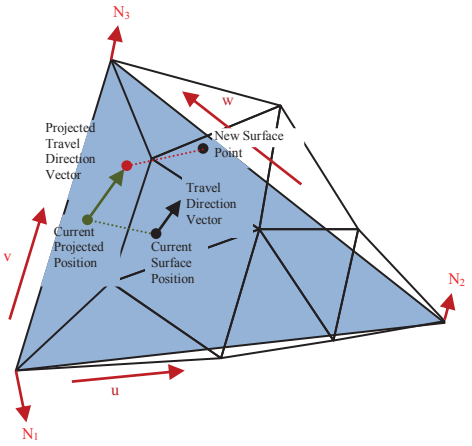

Figure 7. The travel direction vector is computed based on the current surface position. The projected direction vector is applied to the corresponding current position point on the base triangle. The resulting point is then used to compute the new surface point. Dashed lines denote a connection between the points on the base triangle and the curved surface from the Bézier control polygon.

Since the direction vector describes a linear approximation to the motion along the base triangle it becomes worse with increasing curvature which is compounded by distance from the surface. Therefore, to improve stability on a wider range of surfaces while keeping the convergence times small, a gain based on curvature and distance from the surface was used to minimize overshoot when estimating a more accurate contact location. The inclusion of this gain substantially improves the stability and convergence of the system across a variety of object models. Equation 1 shows the computation of this gain where G_o is the overall gain, k is the curvature, d is the finger's distance from the tangent plane, and G_k and G_d are positive factors relating the importance of curvature and distance respectively when computing the next iteration's position. It should be kept in mind that increasing G_k and G_d to increase stability for high curvature models also increases convergence time and thus limits the maximum haptic rate.

$$Gain = \frac{G_o}{(1+G_k k)(1+G_d|d|)} \qquad (1)$$

The distance from the surface (d) is defined as the distance from the current position of the user to the proxy model in contact with the tangent plane. Since arc length increases linearly with radius, the further the user is from the surface the smaller the angle change is needed to align the normal with a particular movement. Thus the gain is reduced linearly by the distance from the surface to ensure that smaller parametric steps are taken.

The curvature (k) is the directional curvature of the surface which is based on the curve formed by intersecting the surface with a normal plane in the travel direction. Since this space curve is not usually in the general arc length parameterized form, the most basic definition of curvature is the magnitude of the rate change of the tangent vector divided by the rate change of position along the curve (see Equation 2). Since the normals defined for each point are not the normals of the Bézier triangle surface, this equation in its pure form cannot be used. However, since by definition, on noncomposite surfaces, the normal vector (N) and the tangent vector (T) are always orthogonal, the magnitudes of their derivatives are also equal. Because we have separate equations for the position (s) and normal vector (N) using barycentric coordinates, and are capable of computing the derivative of each, the final equation used to compute the curvature (k) for our composite surface is the magnitude of the rate change of the normal (N) divided by the rate change in position (s).

$$k = \frac{\|dT\|}{\|ds\|} = \frac{\|dN\|}{\|ds\|} \qquad (2)$$

The derivatives that define curvature (dN and ds) are relatively simple to compute using the chain rule (see Equations 3 to 8). Each of these equations is intended to produce a value used in the following equations, leading eventually to dN and ds. Since barycentric coordinates are homogeneous (u + v + w = 1) only two variables (commonly u and v) are needed to define the system. Depending on the major component of the direction vector, from (u_1, v_1) to (u_2, v_2), one of the two equation sets shown in Equations 3 should be used as the basic derivative to guarantee that $\dot{u}$ and $\dot{v}$ are bounded. The curvature in Equation 2 is scalar invariant with respect to the magnitude of the (u, v, w)

derivative vector, thus both representations are equally valid.

$$\begin{aligned} \dot{v} &= 1 & \dot{u} &= 1 \\ \dot{u} &= \frac{u_2 - u_1}{v_2 - v_1} & \dot{v} &= \frac{v_2 - v_1}{u_2 - u_1} \\ \dot{w} &= -\dot{u} - \dot{v} & \dot{w} &= -\dot{u} - \dot{v} \end{aligned} \quad (3)$$

Next the partial derivatives of position with respect to u, v, and w are computed (see Equations 4). The derivative of position with respect to the system is then computed using chain rule composition (see Equation 5). This derivative is the value of *ds* in Equation 2 when the current barycentric coordinates are plugged in.

$$\begin{aligned} \frac{\partial P}{\partial w} &= P_w = 3(b_{300}w^2 + b_{120}u^2 + b_{102}v^2) + 6(b_{210}wu + b_{201}wv + b_{111}uv) \\ \frac{\partial P}{\partial v} &= P_v = 3(b_{003}v^2 + b_{201}w^2 + b_{021}u^2) + 6(b_{102}wv + b_{012}uv + b_{111}uw) \\ \frac{\partial P}{\partial u} &= P_u = 3(b_{030}u^2 + b_{210}w^2 + b_{012}v^2) + 6(b_{120}wu + b_{021}uv + b_{111}vw) \end{aligned} \quad (4)$$

$$ds = \frac{d}{d(u \text{ or } v)} P = P_w \dot{w} + P_u \dot{u} + P_v \dot{v} \quad (5)$$

All that remains is to compute the derivative of the normal vector before curvature can be calculated. Since the normal vector is divided by its magnitude, the resulting chain form equation is slightly more complicated. Firstly, N and its derivatives are computed (see Equations 6, 7, and 8). Then the derivative of the unit normal can be computed using Equation 8. Finally, the current barycentric coordinates and Equations 5 and 8 are used to compute the curvature (see Equation 2).

$$\begin{aligned} \frac{\partial N}{\partial w} &= N_w = 2(n_{200}w + n_{110}u + n_{101}v) \\ \frac{\partial N}{\partial v} &= N_v = 2(n_{002}v + n_{101}w + n_{011}u) \\ \frac{\partial N}{\partial u} &= N_u = 2(n_{020}u + n_{110}w + n_{011}v) \end{aligned} \quad (6)$$

$$\dot{N} = \frac{d}{d(u \text{ or } v)} N = N_w \dot{w} + N_u \dot{u} + N_v \dot{v} \quad (7)$$

$$dN = \frac{d}{d(u \text{ or } v)} \left(\frac{N}{\|N\|} \right) = \frac{\dot{N}\|N\| - N \frac{N \cdot \dot{N}}{\|N\|}}{\|N\|^2} \quad (8)$$

Once the direction vector is scaled by distance and curvature it is used to define a new set of barycentric coordinates. This is done by adding the scaled direction vector to a point being tracked across the surface of the triangle, and converting the result into barycentric coordinates. This result then becomes the tracked point for the next iteration.

Switching between base triangles is also done at this point. If the tracked point ever leaves the bounds of the current triangle, the focus is switched to the adjacent triangle which shares the crossed edge. The iterations continue as previously as though nothing occurred, only now, the computations use the new triangle. Additional switching needs to be monitored when there is the potential for contacting two nonadjacent triangles simultaneously.

4.5.3 Computing the New Tangent Plane

After the new barycentric coordinates have been computed the error needs to be evaluated to see if more iterations are needed. First the new surface point and normal are computed. The error is defined as the distance between the new tangent and its proxy contact point. The ideal contact point is when the computed surface point and the contact point on the tangent plane are the same (thus error ~0). If the distance between the proxy contact point and computed Bézier surface point is too large (> 1 μm) the process is repeated again using the newly computed tangent plane. The convergence error of 1 μm was chosen to eliminate perceptible artifacts while still allowing reasonable convergence times. With properly tuned gains the system takes, on average, two to three iterations to converge for the objects presented in Section 5.

5 Evaluation Experiments

5.1 Overview of Experiments

Two experiments were run using the 2D (see the Appendix) and 3D (see Section 4) shading algorithms, respectively. The first experiment evaluated several rendering conditions to obtain perceptual thresholds for rendering smooth objects. From the results of the first experiment and the 2D shading algorithm, the 3D algorithm was developed. The second test, involving the 3D algorithm, was used as a means of validating the 3D algorithm and providing further insight into the CLD device's capability to facilitate exploration and shape recognition within a 3D environment. All experiments were conducted with the approval of the University of Utah

Institutional Review Board.

5.2 Smoothness Discrimination of 2D Polygonal Surfaces

5.2.1 Participants

Twelve right-handed individuals (three females) between the ages of 19 and 41 participated in this experiment. None of the participants had prior experience with PHANToMs or the CLD device.

5.2.2 Stimuli

The reference stimulus was a mathematically correct arc segment of a circle (see Figure 8), while the comparison stimulus was a polygonal approximation of the same arc segment. Only the top portion of the circle was haptically rendered. The rendered arc section was 0.902 radians of a 100 mm radius circle, giving approximately 90 mm of travel space. Contact location on the virtual finger was calculated over a 16 mm arc length of the 20 mm radius finger model and linearly mapped to be displayed over 16 mm of travel along the length of the participant's finger.

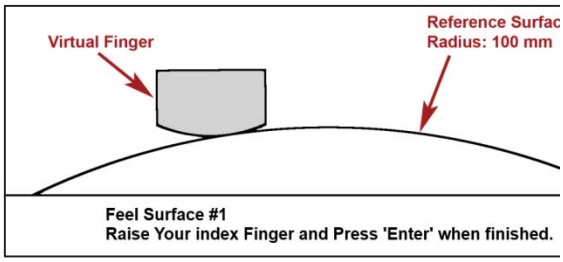

Figure 8. Screen capture of the smooth reference object used during training that preceded each test condition.

5.2.3 Design

Four haptic rendering conditions (C1-C4) were evaluated in order to better understand the requirements for rendering smooth objects when using polygonal models. An adaptive procedure was utilized to assess when participants could no longer distinguish between the polygonal model and the smooth reference surface. These tests were conducted with kinesthetic feedback alone and with combined tactile and kinesthetic feedback. Force (kinesthetic) and tactile shading were also specifically investigated. Forces were rendered using a PHANToM Premium 1.5 while tactile feedback was rendered using the contact location display (CLD) device.

The first two conditions parallel the work by Morganbesser and Srinivasan (1996) and utilize solely kinesthetic force feedback. In these conditions, the contact roller of the contact location display was simply held at the middle of the thimble. Condition 1 (C1) utilized a set of polygons (line segments) to approximate a smooth surface, and did not use any haptic shading. This was done to establish a baseline for the number of segments required for a polygonal model to "feel smooth."

Condition 2 (C2) was identical to Condition 1 (C1), but also included the addition of force shading, as described by Morganbesser and Srinivasan (1996). One slight difference from Morganbesser and Srinivasan (1996) was that we utilized a curved finger model as opposed to a point contact virtual finger model. Completing this experimental condition extends the work described by Morganbesser and Srinivasan (1996) to a more complete state that can be more readily used by hapticians when constructing virtual models of smooth surfaces.

The remaining two conditions utilize the contact location display. Condition 3 (C3) has participants evaluate polygonal models with tactile and kinesthetic feedback (with no shading/smoothing) and the results can be compared to those of Condition 1 (C1) to examine the effect of added contact location feedback.

Condition 4 (C4) had participants utilize tactile and kinesthetic feedback to evaluate polygonal models with tactile shading, but without force shading. This condition was designed to evaluate the influence of tactile feedback and could be compared to all three other conditions. The reason that we did not run our experiment with both tactile and force shading was that we found that this condition resulted in a trivially short experiment during pilot testing (referred to as P1 in Section 5.2.6). That is, participants had difficulty distinguishing the shaded polygonal and perfectly smooth surfaces even when very few polygons were used, and our adaptive procedure would not be appropriate for evaluating this threshold condition. This was to be expected because at 5 line segments there was less than a 0.4% deviation in curvature between the shaded model and the actual smooth surface. Our pilot testing also indicated that adding force shading to force and contact location display (referred to as P2) provided no significant change in sensitivity and was not tested further.

5.2.4 Procedure

The experiment utilized a paired-comparison (two interval), forced-choice paradigm, with a 1-up, 2-down adaptive procedure (Levitt, 1971). On each trial, the participant was presented with two

objects, the smooth reference object and the comparison object with a polygonal representation, in a random order. The participant's task was to indicate which of the two shapes was the smooth object. The number of line segments was decreased after one incorrect response (making the difference between the reference and comparison objects larger, and therefore the task easier) and increased after two consecutive correct responses (making the task more difficult). The threshold obtained corresponds to the 70.7% confidence interval on the psychometric function (Levitt, 1971).

Each condition was conducted as follows. On each trial, the participant would first feel stimulus #1. Once they were finished exploring they would then raise their index finger off the surface and press the 'Enter' key to indicate they were ready for stimulus #2. After feeling the second stimulus they would again raise their index finger and press '1' or '2' and then 'Enter' to indicate which of the two stimuli was the smooth object. Then a new set of comparisons was presented. The order of the reference and comparison stimulus presentation was randomized.

The experiment continued until the participant had finished eleven reversals (a reversal occurred when the number of segments was increased after a decrease, or vice versa). A large step size was used for the first three reversals for a faster initial convergence. A reduced step size was used for the remaining eight reversals for better accuracy in determining the discrimination threshold. The step sizes for each condition were chosen during pilot testing and fixed for all participants in the study.

A Latin Squares reduction of the system was utilized to reduce the number of permutations for balancing testing order in which participants completed the four experimental conditions. The testing apparatus, as shown in Figure 9, was obscured by a cloth cover so that the user would not be able to see either the haptic or tactile device. Instructions were posted on the screen to remind the user where within each comparison they were and how to proceed, but no other visual feedback was provided. White noise was played over headphones to block all auditory feedback, except for audio cues that were provided to indicate the transition between stimuli. Participants were given as much time as they desired to explore each stimulus, but were not permitted to go back to the first stimulus once they had proceeded to the second. It took an average of about forty-two trials and ten minutes to complete each condition per participant.

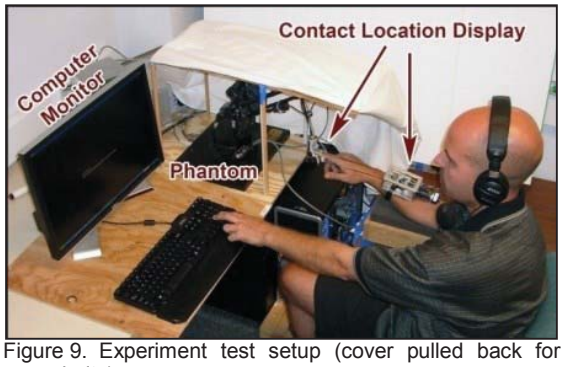

Figure 9. Experiment test setup (cover pulled back for clarity).

5.2.5 *Data Analysis*

Two representative data sets for one participant are shown in Figure 10. Note that this participant had some difficulty in C2 (force feedback with force shading). However, both of these plots still fall within the range of expected participant performance. In all cases, each participant managed to stabilize their performance before completing the eleven reversals. Thresholds were computed as the average of the last 6 reversals.

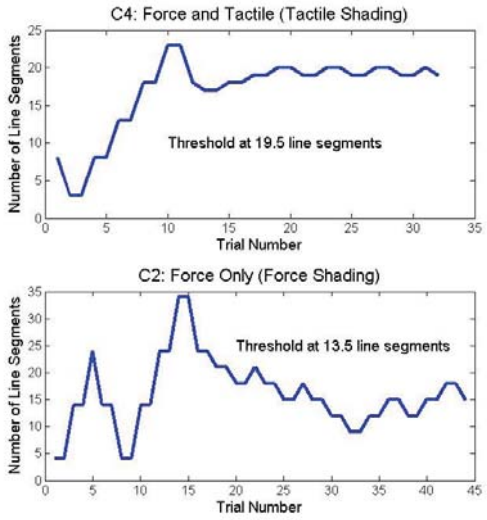

Figure 10. Two collected data plots showing (top) nearly ideal data from one participant and (bottom) less ideal data from the same participant who had difficulty with C2.

5.2.6 *Results*

Table 1 shows the mean discrimination thresholds and the corresponding 95% confidence intervals for the four experimental conditions. While our experiment evaluated the number of polygons needed for a polygonal surface to be indistinguishable from a reference smooth surface, the results are also reported in terms of

the more general metric of the angle difference between adjacent polygonal surfaces. To best understand the practical implications of this data, it is useful to consider this example. If the angle difference between adjacent polygons in a model used exceeds the 95% confidence interval (for example less than 0.37° for C1) then 97.5% or more of people should sense the model as perfectly smooth. Note that the participants were concentrating on the smoothness, so if they were simultaneously engaged in other tasks, these thresholds would increase. Figure 11 plots these means and confidence intervals to visually highlight the significant differences among the four conditions.

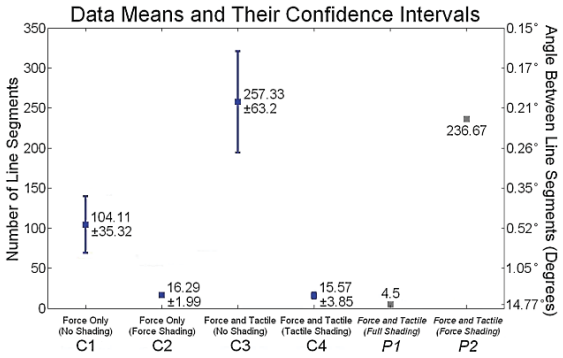

Figure 11. Mean and 95% confidence intervals for each test condition showing the number of line segments at which the polygonal model was indistinguishable from the smooth reference surface. The error bars are not linear when interpreting results based on the angle difference between segments.

The data collected from the twelve participants passed an omnibus ANOVA test [$F(44,47) = 47.76$, $p < 0.001$]. This implies independence between all four conditions and allows the use of Tukey's test to determine if the results are significantly different. The data were subsequently analyzed for statistically significant differences using Tukey's test with $\alpha = 0.05$. The average number of line segments for each threshold was the highest for C3 (257.3), followed by that for C1 (104.1), and the lowest for C2 and C4 (16.3 and 15.6, respectively). It was found that C3 (force and tactile rendered) was significantly different from all other conditions. C1 (force only rendered) was also significantly different than all other conditions. The two shading conditions (C2 and C4) were not significantly different from each other.

Table 1. Means and 95% confidence intervals for all four test conditions, showing the number of line segments needed for a polygonal surface to be indistinguishable from the smooth reference surface and the corresponding angle difference between adjacent line segments in degrees (in parentheses).

	C1 Force Only	C2 Force Only with Force Shading	C3 Force and Tactile	C4 Force and Tactile with Tactile Shading
Mean	104.1 (0.5°)	16.3 (3.4°)	257.3 (0.2°)	15.6 (3.5°)
95% Confidence	± 35.32 (+0.25°, -0.13°)	± 1.99 (+0.44°, -0.35°)	± 63.20 (+0.07°, -0.04°)	± 3.85 (+1.09°, -0.66°)

As mentioned earlier, a more general and useful metric that can be taken from our results is the angle difference between adjacent polygons, as this can be applied to other generic polygon models. This measure corresponds to the way discontinuities between line segments connect. This concept is similar to that proposed by Morganbesser and Srinivasan (1996) with one important distinction: the tactile feedback is felt as short rolling bursts as the user crosses the vertexes, due not only to the instantaneous changes in force direction but also changes in the geometric shape itself (e.g., angle differences between adjacent polygons). Table 1 shows the angle difference thresholds corresponding to the line-segment thresholds in parentheses. The same angle differences are shown in Table 2 where test conditions are organized according to rendered and shaded variables. Two additional threshold values are shown from pilot testing (P1 and P2, collected from two participants) for comparison and discussion later.

Table 2. Estimated mean angle difference, in degrees, between adjacent line segments to create a curved surface that feels smooth.

	Rendered Condition	
	Force Only	Force and Tactile
No Shading	0. 5° (C1)	0. 2° (C3)
Force Shading	3. 4° (C2)	0. 2° (P2)
Tactile Shading	NA	3. 5° (C4)
Force and Tactile Shading	NA	14. 8° (P1)

5.2.7 Discussion

Our results are not directly comparable to that of Morganbesser and Srinivasan (1996), as these researchers only tested to show improvements in perceived smoothness and explored coarse models using up to three polygons. However, it is interesting to compare C1 to prior work on discriminating the angle difference between sequentially applied force vectors. Barbagli et al. reported a discrimination threshold of 28.4° for sequentially applied force vectors (Barbagli, Salisbury, Ho, Spence, & Tan, 2006), which is nearly two orders of magnitude larger than the thresholds we report for the instantaneous changes in force orientation experienced in C1 (0.5°). This is not surprising though as people have much greater sensitivity to changes presented in rapid succession (Gescheider, 1997). Our task also utilized active rather than passive sensing in making perceptual judgments, which is also expected to provide greater perceptual sensitivity (Klatzky & Lederman, 2003). Frisoli, Solazzi, Reiner, and Bergamasco (2011) performed an experiment involving both force and tactile feedback which demonstrated the addition of tactile feedback increased user ability to detect small angle differences between nearly parallel planes. Frisoli et al. reported a perception threshold ranging from 0.7° with force and tactile feedback to 2.6° with force feedback only. Since our task involved detecting the edge formed from the two planes rather than detecting a change in force direction we would expect our results to show lower perception thresholds (our results showing 0.2° to 0.5° thresholds under the same feedback conditions).Several trends can be observed from the data presented in Table 1 and Table 2. First of all, the addition of tactile feedback greatly increases one's sensitivity to edges and vertices in the system, as seen by pair-wise comparisons of the thresholds for C1 and C3 and those for C2 and P2 in Table 2. This increased sensitivity is undesirable when rendering smooth surfaces as it requires more line segments causing an increase in computation time and a decrease in rendering performance. Fortunately, force and/or tactile shading can decrease one's sensitivity to edges and vertices, as seen by the significant difference found between the thresholds for C1 and C2 and those for C3 and C4. This significant difference shows that both the force shading algorithm, developed by Morganbesser and Srinivasan, and our 2D shading algorithm (presented in the Appendix), significantly reduce the needed number of line segments to make a polygonal object feel smooth. Further, it is not practical to provide tactile feedback for polygonal object models without our shading algorithm, as indicated by P2. Note that in C4 the 2D shading algorithm did not smooth forces. Therefore, the threshold of 3.5° can be further improved (in terms of decreased number of line segments) by employing force shading, as indicated by the threshold of 14.8° for P1 shown in Table 2.

Another interesting observation is that people appear to rely more on tactile than force information to judge the smoothness of a surface. Participants judged polygonal surfaces in C4 to be smoother based on shaded tactile feedback, even though normal force discontinuities still existed to the same degree as in C1. This indicates that the tactile sensations may carry more weight in the haptic perception of smoothness than the force irregularities. In fact, in the presence of unshaded tactile information (see C3 and P2 in Table 2), there appears to be no significant benefit from applying Morganbesser and Srinivasan's force shading algorithm.

In summary, the use of shading algorithms can lead to a significant reduction in the size of polygonal models by approximating smooth object surfaces without introducing noticeable artifacts. Very small angle differences between adjacent polygons (0.2-0.5°) were required for rendering smooth objects when shading was not used. Thus, large numbers of polygons were needed for these models to feel smooth. The addition of force and/or tactile shading significantly reduced the required model size as can be seen in Figure 11 and Table 2. Either form of force (C2) or tactile (C4) shading allowed a relatively large angle difference between polygons (~3.5°, a factor of 6 over unshaded conditions), while our pilot tests (P1) showed greater angle differences between polygons (~15°, a factor of 30 over unshaded conditions) were possible if both force and tactile shading was simultaneously applied, thereby requiring a significantly smaller number of polygons to represent a given smooth haptic model. This can clearly have a huge impact on reducing the necessary size of a haptic model, without sacrificing the fidelity of the haptic interaction. Although our results were obtained with the contact location display (in C3 and C4), the angle difference thresholds are likely applicable to other types of tactile displays including those that render the tangent lines of a curved surface (Dostmohamed & Hayward, 2005; Frisoli et al., 2005).

5.3 Identification of 3D Object Shapes

5.3.1 Participants

Seventeen right-handed individuals and one left-handed individual (two females) between the ages of eighteen and thirty-eight participated in the experiments. The participants were divided into two groups: experienced and inexperienced. Experienced participants took part in the 2D experiment described in Section 5.2. Inexperienced participants had no prior experience with the CLD device but some had prior experience with other haptic devices. There were nine experienced and nine inexperienced participants, respectively.

5.3.2 Stimuli

Seven objects were selected for this experiment during pilot testing as being distinct, while providing opportunity for confusion between similarly shaped objects, depending on the rendering conditions. These seven primitives are the cone, cylinder, cube, sphere, tetrahedron, extruded octagon, and extruded triangle (see images in Table 3). Each object fit within a 40 mm radius cylinder and was 80 mm long with the exception of the cube which was 56.6 mm long. The orientation of these objects was fixed for all models in the experiment with the primary axis as horizontal and from the left to right. Participants were not informed of the model orientation to prevent exploration strategies involving finding a particular feature. The cone and tetrahedron models are asymmetric along this axis and could provide directional information. These models were rendered facing either direction (pointed to both left and right) during the experiment to eliminate the direction cue.

The 1-DOF gimbal on the CLD was modified from the first experiment (Section 5.2) to allow additional motion from side-to-side although only the tilt angle was monitored. The user's finger orientation was limited to pointing forward and tilting up and down.

5.3.3 Design

Virtual objects were rendered under four experimental conditions. The tests were conducted with either kinesthetic feedback alone or with combined tactile and kinesthetic feedback. Kinesthetic feedback was provided by a PHANToM device and tactile feedback was provided by a 1-DOF CLD device. Object models were rendered with or without haptic shading. The former case created smooth curved objects and rounded the edges of flat-sided objects such as cubes. Rounded corners with a radius of 1.5 mm were implemented as suggested at the end of Section 4.3 through the inclusion of extra triangles. See (Doxon, 2010) for further rendering details.

The addition of rounded edges was expected to allow the user to better maintain contact with the object's surface and thus improve object recognition. Loss of contact with objects was a problem that hampered participants' ability to identify simple object shapes as previously reported by Frisoli et al. (2005). Objects containing smooth curved surfaces (cone, cylinder, and sphere) were rendered as high count polygonal representations when haptic shading was not used.

5.3.4 Procedure

A blocked design was utilized for this experiment. Each participant performed a total of eight runs across two sessions, containing four runs each. Each session was separated by at least a day. Within each run the participant was presented with all seven objects as both shaded and unshaded models to identify. Each of the fourteen object models was presented once per run, and the order in which they were rendered was chosen randomly. Two runs (a block) were conducted back to back with the same stimulus set. Shapes containing directional information (cone and tetrahedron) were rendered facing either left or right and chosen such that across each session both directions were experienced under each rendering condition.

The first half (two runs) and second half (two runs) of each session differed in whether tactile feedback was rendered or not. Even numbered participants evaluated the first half of the experiment with tactile and kinesthetic feedback and the second half with only kinesthetic feedback, while odd numbered participants performed the opposite. When no tactile feedback was rendered, the CLD device was commanded to a position at the center of the thimble and remained in contact with the participant's finger to ensure a purely kinesthetic interaction.

In each trial the participant explored the currently rendered object and identified it from the list of seven objects provided to them (see Table 3). The participant was instructed to press the number key corresponding to the identified shape, e.g., “4” for a sphere. The response and timing data were recorded and the participant was guided back to the starting position by weak attractive forces and visual feedback of the finger

position. Participants were required to remain at the starting position for one second before continuing. This helped the participant to begin each trial at the same relative location above each virtual object. At the end of the one second period, a "ding" sound was played and visual feedback disappeared to prompt the participant to begin exploring the next object to be identified. The experiment continued until all fourteen objects in a run were identified. A short break was given between the second and third runs in a session while the CLD device was adjusted for use in a different feedback condition, which involved the addition or elimination of tactile (CLD) feedback.

Before the test data was recorded for each feedback condition, the user was allowed to interact with an extruded hexagon for practice. Visual feedback showing the virtual object and the user's virtual finger on the LCD was provided to the user during the practice. However, no such visual cues were provided during the main experiment, except for the visual cues that guided the user to raise their finger back above the virtual objects after each response.

The same testing apparatus that was used during the 2D experiment (see Figure 9) was also used in the 3D object recognition experiment. A cloth cover was used to stop the user from being able to see either the haptic or tactile device. A list of the seven objects and their corresponding numbers was provided to the participants on a sheet of paper but no further instructions were posted on the screen. White noise was played over headphones to block all auditory cues except those provided by the program to indicate a transition between trials. Participants were given as much time as they desired to explore the objects but were instructed to respond as quickly as they felt comfortable. Participants were not permitted to change their responses once given.

5.3.5 Data Analysis

Trials from all participants were pooled and organized into a stimulus-response confusion matrix with rows representing stimulus and columns representing responses. This matrix was further broken into two to show each combination of rendering conditions. These matrices were used to evaluate percent correct scores and pair-wise confusions as well as response time data. Only response times from correct answers were used to determine average response times.

5.3.6 Results

5.3.6.1 Accuracy

Figure 12 shows the number of correct answers given by participants for each of the seven different objects. Objects were identified with a mean accuracy of 81.9% and a standard deviation of 10.0%. This matches the results found in Kirkpatrick and Douglas (2002) where a similar object identification task was performed (mean 84%, deviation 12%). Jansson and Monaci (2006) found an accuracy of around 70% when exploring real objects with a plastic shell placed over the finger tip. This relatively high percent-correct score indicates that a performance ceiling may have been reached, making it difficult to observe any performance improvement in accuracy due to the additional tactile (CLD) cues. Of the seven shapes, the extruded triangle was the most difficult to identify at a 68.4% accuracy and the sphere was the easiest at a 97.6% accuracy. These values can also be computed from the diagonal cells of Table 3.

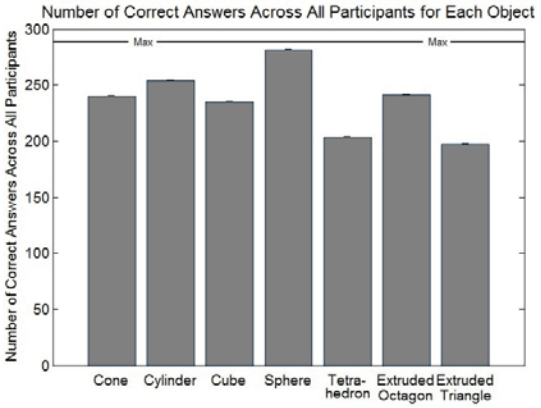

Figure 12. *Total number of correct answers* given by all participants for each of the seven objects.

Table 3 shows the stimulus-response confusion matrix in percent-correct scores pooled from all participants. The rows represent the stimulus shapes presented to the participant while the columns represent the responses. The diagonal cells containing correct answers have been highlighted. Significant off diagonal terms have been bolded and shaded. Compared to a chance performance level of 14.3% (1/7) correct, the overall accuracy was relatively high, indicating that the participants were able to disambiguate the seven test stimuli reasonably well. The off-diagonal cells in Table 3 are asymmetric, which implies that participants perceived some objects as others but not vice versa. The most predominant confusion was

identifying the tetrahedron as a cone (20.1% of the total trials) and to a lesser extent the cone as a tetrahedron (8.3% of the total trials).

Table 3. Confusion matrix showing percent accuracy for *all participants*. The diagonal has been highlighted in black. Major confusion values have been highlighted in grey.

Shape Presented to Participant	Shape Identified by Participant						
	83.3	**4.5**	0.3	1.7	**8.3**	0.3	1.4
	1.7	**88.2**	**5.9**	0	1.0	1.7	1.4
	2.1	3.1	**81.6**	2.1	0.7	**4.9**	**5.6**
	0.3	0.7	0	**97.6**	0.3	1.0	0
	20.1	0.3	0.3	3.8	**70.5**	1.0	3.8
	1.0	**6.9**	3.5	0	1.7	**83.7**	3.1
	2.4	4.2	3.8	0.7	**10.1**	**10.4**	**68.4**

Weaker (< 10%) but still predominant confusions were also observed. Participants confused the extruded octagon with the cylinder (6.9% of the total trials) more often than vice versa (1.7% of the total trials). The extruded triangle was confused for the tetrahedron (10.1% of the total trials), which contains a similar shape and orientation. While all the listed confusions so far are between elements with similar geometry, the confusion between the extruded triangle and the extruded octagon (10.4% of the total trials) was unexpected. One reason for this confusion may have been that the extruded triangle's faces are nearly vertical which makes them more difficult to interact with. Participants may have been identifying the shape as an extruded octagon by the orientation of the faces alone rather than fully comprehending the overall shape of the model.

To the least extent there were small confusions involving the cone identified as a cylinder (4.5% of the total trials), the cylinder identified as a cube (5.9% of the total trials), and the cube identified as an extruded octagon (4.9% of the total trials) and extruded triangle (5.6% of the total trials). These confusion elements constitute less than 6% of the total number of trials for each object.

Effect of haptic shading. The confusion matrix shown in Table 3 was split into two matrices according to whether the object's edges were rounded. It was found that shading had no effect on the confusion of the tetrahedron with other objects, between the extruded triangle and the extruded octagon, or the confusion of the cylinder as the cube.

However, the extruded octagon was predominantly confused for the cylinder when its edges were rounded (shaded), whereas the following confusions mainly occurred with unshaded objects: the extruded triangle as the tetrahedron, and the cube as either extruded octagon or triangle. Overall, there was not a significant difference found in accuracies between objects with and without rounded edges [$t(502) = 1.53$, $p = 0.1277$].

Effect of CLD. The confusion matrix shown in Table 3 was subdivided into two matrices to examine the effect of additional contact location feedback on object recognition. The percent-correct scores were 82.5% and 81.3% for the kinesthetic alone and combined kinesthetic and tactile feedback cases, respectively. Neither the identification accuracy nor response time were significantly different. Jansson and Ivas (2001) indicated that the potential usefulness of a device may be underestimated when inexperienced users are evaluated. The potential ceiling effect coupled with the fact that the majority of users were not explicitly trained on the device could explain the lack of significant difference. This was somewhat in contrast with our findings in the first experiment reported in Section 5.2.

Effect of user experience. The confusion matrix in Table 3 was also divided into two matrices for the experienced and inexperienced participants. The overall percent-correct scores for the experience and inexperienced participants were 87.5% and 76.3%, respectively. Experienced participants were significantly more accurate than inexperienced participants [$t(250) = -4.01$, $p < 0.0001$]. While the weaker confusions were not present for the experienced users, both groups had the same level of difficulty identifying the extruded triangle.

5.3.6.2 Response Time

Two types of response times were collected within each trial. The first of these began counting as soon as the object was touched and haptic forces were rendered. The second gathered response time counted only during the times when the user was in contact with the surface of the object. Both response times stopped counting when a response was given. This response time data provides additional measures of the difficulty of the object identification task. Figure 13 shows the mean times between the start of a trial and when a participant responded for all seven objects. The average response time varied from 8.6 s (sphere) to 18.7 s (extruded triangle),

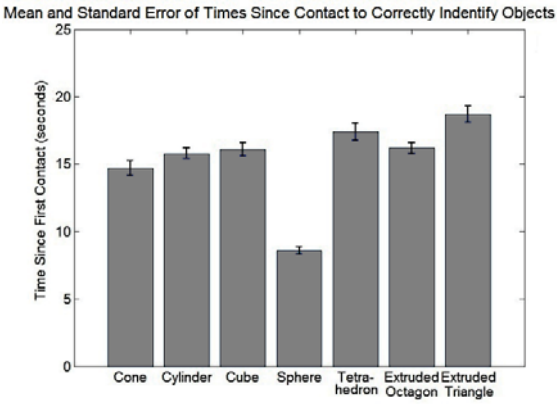

Figure 13. Time since initial contact till response for each of the seven objects.

with the sphere taking only about half the amount of time to identify as any of the other six objects [$t(1649) = -10.10$, $p < 0.0001$] and being significantly more accurately identified [$t(250) = -4.62$, $p < 0.0001$]. This was as expected because of the sphere's unique geometric profile among the seven objects. Kirkpatrick's 2002 object identification task provided similar identification times of 22.4 seconds.

Effects of haptic shading. The effect of shading on object recognition time can be seen in Figure 14 where the percent of time in contact with the object under the shaded and unshaded conditions is shown, respectively. It can be seen that rounded edges on objects allowed participants to stay in contact with the object's surface for a larger portion of the total object-exploration time for each of the seven stimulus objects [$t(1649) = 37.14$, $p < 0.0001$]. However, as mentioned earlier, the longer contact time for shaded objects did not result in a significantly higher object-recognition accuracy level.

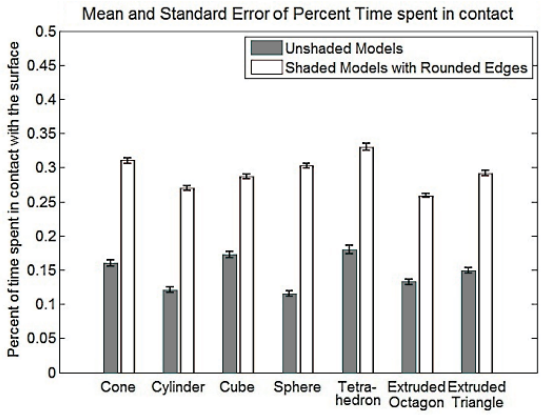

Figure 14. Effect of shading on the percent time spent in contact with objects.

Effect of user experience. Response time data for experienced and inexperienced users was compared. Experienced users were found to be universally faster at identifying the objects [$t(1649) = -5.92$, $p < 0.0001$]. All objects showed a significant difference in identification time except the extruded octagon and tetrahedron. Experience made the largest time difference on the extruded triangle.

5.3.7 Discussion

The results of the 3D object recognition experiment showed that the participants were able to identify seven common geometric shapes with an accuracy of above 80% correct with force and contact location information. With this relatively high recognition rate, we might have hit a ceiling effect that made it difficult for the participants to demonstrate any additional benefit of 3D shading of object edges or contact location information. More detailed analysis of the confusion matrices showed that while shading reduced confusions between objects for some shapes (e.g., misrecognition of cubes as extruded triangles or extruded octagons), it did not significantly affect the recognition accuracy for tetrahedrons. Moreover, shading appeared to have contributed to increased confusion of extruded octagons as cylinders. Some of these results are as expected. For example, users likely had a difficult time following the contours of the cube while it was unshaded. The addition of rounded edges eliminated this problem and therefore made cubes more distinguishable from extruded triangles or extruded octagons. Other results, such as that for the tetrahedron, appear to suggest that tetrahedrons are generally difficult to recognize with the experimental setup used in the present study.

Our results showing that the addition of rounded edges significantly increased the percentage of time spent in contact with virtual objects are consistent with those of other studies. For example, Frisoli et al. previously reported that loss of contact with objects hampered their subjects' ability to identify simple object shapes (Frisoli et al., 2005).

Users with prior experience with the CLD device identified objects faster and with higher accuracy than those without. This finding indicates that, like other haptic devices, the CLD device required some practice before it can be used to its fullest potential.

Independently, participants seemed to develop a common exploration strategy. This strategy involves first moving left and right to

determine whether there are sides on the object. This was done using only kinesthetic information due to finger orientation and the CLD device characteristics. This immediately determines which of three groups the object falls into: 1) the sphere, 2) the cone and tetrahedron, and 3) the cylinder, cube, extruded octagon, and extruded triangle. Participants then returned to the center of the object and explored forward and backward to identify the object from within the subgroup. This exploration strategy explains the faster speed and better accuracy in identifying the sphere as it is unique in the left-right direction. The strategy also indicates why potential confusion may have occurred on the extruded triangle and tetrahedron which both contain only an edge along the top.

It was expected that the use of the CLD device would decrease confusion among the objects due to the additional tactile cues. The results show that while there is no statistical difference between the number of correct answers given with and without tactile feedback, the majority of the off-diagonal confusion cells identified earlier in Table 3 are more uniformly distributed when tactile feedback is presented, indicating less overall confusion. While the tactile cues might have assisted the participants in object recognition, user's interactions with the CLD device suggest that further mechanical revisions are required before the CLD can provide more effective haptic interactions in 3D environments. This was especially noticeable when using the CLD to contact the front or bottom faces of objects. In this situation the dynamics of the device bend the spring steel drive wires away from the user's finger and conflicts with the intended haptic interaction. Therefore, whatever benefits the CLD device provided might have been degraded by the limitations in its mechanical design.

6 Conclusions and Future Work

We have presented haptic shading algorithms that make it possible to fully utilize the contact location display (CLD) device with polygonal object models. These algorithms can also be used with other haptic systems with combined tactile and kinesthetic feedback. Haptic shading algorithms for both 2D and 3D environments were developed. Both algorithms create perceptibly smooth haptic interactions allowing a significant reduction in the size of complex models. These algorithms can serve as a replacement to Morganbesser and Srinivasan's (1996) force-shading algorithm for a range of haptic devices. Each haptic shading algorithm was evaluated experimentally.

The experimental results are intended to be used as a guide to utilizing haptic shading to its fullest extent. The rendering thresholds provided through the first experiment state the level of detail haptic models needed in order to feel smooth when rendered with general kinesthetic and/or tactile rendering systems. The first experiment, utilizing the 2D algorithm, evaluated the perception thresholds for angle difference between adjacent polygons under four cases: unshaded force rendering, shaded force rendering, unshaded force and tactile rendering, and shaded tactile with unshaded force. The addition of tactile feedback through the CLD device significantly increased the ability of users to detect an edge from 0.5° to 0.2° angle difference between adjacent polygons. The inclusion of shading in both tested conditions substantially decreased the perception threshold and allowed then angle between adjacent polygons to increase to ~3.5°. The full shading algorithm was found to reduce this further allowing up to ~15° angle difference between adjacent polygons before model discontinuities became noticeable.

A second experiment, utilizing the 3D algorithm, evaluated the CLD device's capability to facilitate dexterous exploration and shape recognition. This experiment demonstrated the efficiency of our 3D algorithm, but points out design flaws in the current CLD device.

Our experiments indicate that the CLD device should be revised before conducting further tests in 3D environments. Such a redesign will permit research into grasping and manipulation. The next revision of the device may need to apply kinesthetic feedback through the thimble rather than through the contact element (roller) of the CLD device. After redesigning the device to make it more effective within 3D environments there may be a more noticeable improvement in user capabilities to identify objects rendered with contact location feedback.

7 Acknowledgements

This work was supported, in part, by the National Science Foundation under awards IIS-0904456 and IIS-0904423. The authors thank Jaeyoung Park for suggesting a more concise method of expressing the angular fraction used within the 2D algorithm (see Appendix).

8 REFERENCES

[1] Barbagli, F., Salisbury, K., Ho, C., Spence, C., & Tan, H. Z. (2006). Haptic discrimination of force direction and the influence of visual information. In ACM Transactions on Applied Perception, Vol. 3, No. 2, pp. 125 - 135, 2006.

[2] Cohen E., Riesenfeld R., & Elber, G. (2001). Geometric modeling with splines: an introduction. Mass: AK Peters, Chapters 5 - 11, 2001.

[3] Daniels, J., Silva, C. T., Shepherd, J., & Cohen, E. (2008). Quadrilateral mesh simplification. In ACM SIGGRAPH Asia 2008 Papers, Singapore, 2008.

[4] Dostmohamed, H. & Hayward, V. (2005). Trajectory of Contact Region On the Fingerpad Gives the Illusion of Haptic Shape. In Experimental Brain Research, Vol. 164, No. 3, pp. 387 - 394, 2005.

[5] Doxon, A. (2010). Force and Contact Location Shading Methods For Use Within Two and Three Dimensional Environments. Master's Thesis. UMI Order Number: AAT1478013, The University of Utah, 2010.

[6] Frisoli, A., Bergamasco, M., Wu, S., & Ruffaldi, E. (2005). Evaluation of multipoint contact interfaces in haptic perception of shapes. Multi-point interaction with real and virtual objects. Springer Tracts in Advanced Robotics, Vol. 18, pp. 177 - 188, 2005.

[7] Frisoli, A., Solazzi, M., Salsedo, F., & Bergamasco, M. (2008). A fingertip haptic display for improving curvature discrimination. Presence: Teleoperators and Virtual Environments, Vol. 17, No. 6, pp. 550 - 561, 2008.

[8] Frisoli, A., Solazzi, M., Reiner, M., & Bergamasco, M. (2011). The contribution of cutaneous and kinesthetic sensory modalities in haptic perception of orientation. Brain Research Bulletin 85, pp. 260 - 266, 2011.

[9] Fritschi, M., Ernst, M., & Buss, M. (2006). Integration of kinesthetic and tactile display – a modular design concept. In 2006 EuroHaptics Conference, 2006.

[10] Gescheider, G. A. (1997). Psycophysics: The Fundamentals. 3rd ed: Lawrence Erlbaum Associates, New Jersey, 1997.

[11] Jansson, G. & Monaci, L. (2006). Identification of real objects under conditions similar to those in haptic displays: providing spatially distributed information at the contact areas is more important than increasing the number of areas. Virtual Reality, Vol. 9, No. 4, pp. 243 - 249, 2006.

[12] Jansson, G. & Ivas, A. (2001). Can the Efficiency of a Haptic Display Be Increased by Short-Time Practice in Exploration?. Proceeding of Haptic Human-Computer Interaction Workshop, September 2001.

[13] Johnson, D. & Cohen, E. (1999). Bound coherence for minimum distance computations. In Proceedings of IEEE International Conference on Robotics and Automation, pp. 1843 - 1848, 1999.

[14] Kirkpatrick, A. & Douglas, S. (2002). Application based evaluation of haptic interfaces. In Proceedings of the Tenth Symposium on haptic interfaces for virtual environment and teleoperator systems, 2002.

[15] Klatzky, R. & Lederman, S. (2003). Touch. In A. F. Healy and R. W. Proctor, editors, Handbook of Psychology, volume 4: Experimental Psychology, chapter 6, pp. 147 - 176. John Wiley and Sons, 2003.

[16] Kuchenbecker, K., Provancher, W., Niemeyer, G., & Cutkosky, M. (2004). Haptic display of contact location. In Proceedings of the IEEE Haptics Symposium, pp. 40 - 47, 2004.

[17] Levitt, H. (1971). Transformed up-down methods in psychoacoustics. In Journal of the Acoustical Society of America, Vol. 49, pp. 467 - 477, 1971.

[18] McNeely, W., Puterbaugh, K., & Troy, J. (1999). Six degree-of-freedom haptic rendering using voxel sampling. In Conference on Computer Graphics and Interactive Techniques (SIGGRAPH 1999), pp. 401 - 408, 1999.

[19] Morganbesser, H. & Srinivasan, M. (1996). Force shading for shape perception in haptic virtual environments. In Proceedings of the 5th Annual Symposium on Haptic Interfaces for Virtual Environment and Teleoperator Systems, ASME/IMECE, Atlanta GA, DSC:58, 1996.

[20] Phong, B. (1973). Illumination for Computer-Generated Images. Doctoral Thesis. UMI Order Number: AAI7402100, The University of Utah, 1973.

[21] Provancher, W., Cutkosky, M., Kuchenbecker, K., & Niemeyer, G. (2005). Contact location display for haptic perception of curvature and object motion. International Journal of Robotics Research, Vol. 24, No. 9, pp. 691 - 702, 2005.

[22] Provancher, W. & Sylvester, N. (2009). Fingerpad Skin Stretch Increases the Perception of Virtual Friction. In IEEE Transactions on Haptics , Vol. 2, No. 4, pp. 212 - 223, Oct - Dec, 2009.

[23] Ruspini, D. & Khatib, O. (2001). Haptic display for human interaction with virtual dynamic environments. Journal of Robotic Systems, Vol. 18, No. 12, pp. 769 - 783, 2001.

[24] Ruspini, D., Kolarov, K., & Khatib, O. (1997). The haptic display of complex graphical environments. In Computer Graphics and Interactive Techniques (SIGGRAPH 1997), pp. 345 - 352, 1997.

[25] Salada, M., Colgate, J., Vishton, P., & Frankel, E. (2005). An experiment on tracking surface features with the sensation of slip. WHC 2005. First Joint EuroHaptics Conference and Symposium on Haptic Interfaces for Virtual Environment and Teleoperator Systems, pp. 132 - 137, 2005.

[26] Seong, J. K., Johnson, D., Elber, G., & Cohen, E. (2010). Critical point analysis using domain lifting for fast geometry queries. In the Journal of Computer-Aided Design, Vol. 42, No. 7, pp. 613 - 624, 2010.

[27] Thompson II, T. & Cohen, E. (1999). Direct haptic rendering of complex trimmed NURBS models. In Proceedings of Haptic Interfaces for Virtual Environment and Teleoperator Systems, ASME, 1999.

[28] Vlachos, A., Peters, J., Boyd, C., & Mitchell, J. (2001). Curved PN triangles. In Symposium on Interactive 3D Graphics, pp. 159 - 166, 2001.

[29] Webster, R., Murphy, T., Verner, L., & Okamura, A. (2005). A novel two-dimensional tactile slip display: design, kinematics and perceptual experiments. ACM Transactions on Applied Perception, Vol. 2, No. 2, pp. 150 - 165, 2005.

9 APPENDIX: 2D HAPTIC SHADING ALGORITHM

9.1 Overview of the 2D Haptic Shading Algorithm

The 2D haptic shading algorithm creates a smooth haptic interaction given a 2D polygonal model. This is done by calculating a series of quadratic Bézier curves to create a new smooth curve based on the shape of the original polygonal model, which is then used to compute contact positions and rendered forces. This makes the underlying facets of the model imperceptible and allows a substantial reduction in model complexity while still retaining proper contours.

Rather than interacting with the Bézier curve

directly, this approach computes a dynamically updated tangent line at the point of contact. To guarantee the resulting smooth curved surface is continuous, all defined vertices must be connected in a single polygon. Multiplicity, or multiple points defined at the same coordinates, can be used to generate sharp corners on the rendered smooth surface when desired.

While the algorithm was developed to provide both smooth tactile and kinesthetic feedback it can be used as a substitute for the methods presented by Morganbesser and Srinivasan (1996) for force shading.

An example rendered smoothed surface for an arbitrary polygonal model shown in Figure 15. The dashed black lines represent the original polygonal model and the thick curve represents the shape of the resulting curved surface. The grey shaded regions show the extent of each Bézier patch as well as a local parameterization used in the algorithm. The overall shape is built from these patches.

9.2 Bezier Curves

The 2D haptic shading algorithm utilizes a quadratic Bézier curve for each of its patches. Quadratic Bézier curves are defined by a control

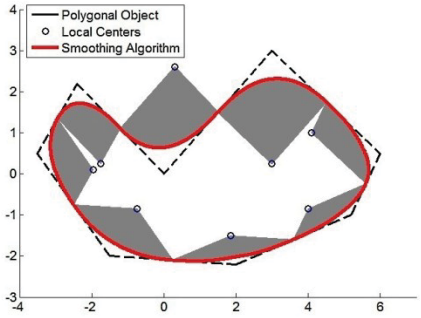

Figure 15. The original polygonal model (dashed black) and the smooth interaction model (thick curve). Separate Bézier patches are defined across each region denoted by the grey regions.

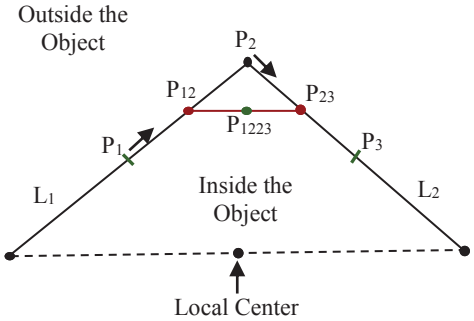

Figure 16. Basic labeling scheme used in our 2D shading algorithm.

polygon containing three ordered points and have two valuable properties that help define the generated control polygon. First, the end points of the resulting Bézier curve are the end points of the control polygon (Cohen et al., 2001). Second, the quadratic Bézier curve is tangent to its control polygon at the end points (Cohen et al., 2001). These properties are used to guarantee that the resulting surface is smooth and contiguous.

The de Casteljau algorithm is an elegant constructive algorithm that computes a point and tangent on the Bézier curve based on a single parameter value, t (Cohen et al., 2001). Varying the parameter value from 0 to 1 traces out the Bézier curve. The de Casteljau algorithm allows us to directly compute the tangent line for any given value of t. Equations 9 define the two points that make up this tangent line.

The labels used in these equations correlate to those shown in Figure 16. The point subscripts help to denote the location of the point. The two line segments that are adjacent to the vertex of interest are labeled L_1 and L_2. The arrows denote the direction that the points P_{12} and P_{23} will travel for increasing values of t. The local center is an integral part of the radial parameterization used by the algorithm.

$$P_{12} = P_1(1-t) + P_2 t$$
$$P_{23} = P_2(1-t) + P_3 t \qquad (9)$$

9.3 Preparing the Model

9.3.1 Defining the Control Polygon

In order to retain tangent continuity over patch boundaries, our algorithm forms a separate Bézier patch for each vertex on the original model. The control polygon is defined as the vertex and the midpoints of each line segment connected to it. Figure 17 shows three tangent line segments at t = 0.25, 0.50, and 0.75 for each Bézier patch. The adjacent midpoints used are shown as ticks.

Additionally, a single local center needs to be defined for each Bézier patch. This local center will be used to compute the new parameter value t in the algorithm. The local center cannot be located on L_1, L_2, or the resulting curve. While the local center may be placed almost anywhere, ideally it should be placed at the center of curvature of L_1 and L_2. The center of curvature can be found by computing the intersection of lines perpendicular to L_1 and L_2 placed at their respective midpoints. Placing the local center at

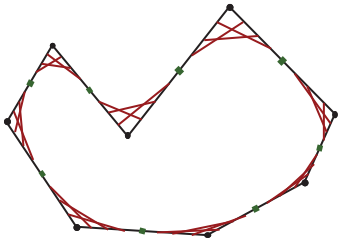

Figure 17. An arbitrary polygonal shape. Three tangent line segments are shown for each Bézier patch at t = 0.25, 0.50, and 0.75. Only one tangent will be in existence at a single instant in time.

the center of curvature of the polygonal lines ensures the highest numerical precision. Another convenient location for the local center is at the midpoint of the ends of L_1 and L_2 opposite the shared vertex, as used in Figure 17.

9.4 Implementing the 2D Haptic Shading Algorithm

The next few sections cover each step of the 2D haptic shading algorithm in detail.

9.4.1 Computing the Current Proxy Contact Location

To begin each iteration, the finger is projected into contact with the current tangent line. When moving, this contact position represents a small differential distance along the tangent line and thus is a reasonable first approximation for determining the user's current position on the surface. No forces need to be computed or applied during this step.

9.4.2 Computing the New Parameter Value t

From the new contact location, a parameter value t can be computed. Finding the parameter value of the Bézier curve that corresponds to the ideal contact point on the quadratic curve is difficult and slow. Instead, the parameter value is approximated through a radial parameterization, which slightly alters the shape of the resulting surface.

The first step in approximating the new parameter value t is to determine which Bézier patch to use. That is, determine the current L_1 and L_2 lines. These lines are likely the same ones as those from the previous iteration. There are two conditions that will cause new lines to be selected. The first of these conditions is when multiple contact points exist on nonadjacent line segments. The second condition occurs frequently just as the user passes over the midpoint of L_1 or L_2. At this point a new vertex is now closer to the contact point, and its corresponding line segments become the new L_1 and L_2. The corresponding local center for the new Bézier patch is used.

Once L_1 and L_2 have been identified, all that is left is to compute the corresponding parameter value. This is done directly by computing the angular fraction (t=α/β) between the current contact point and the start of the curve with respect to the local center. In Figure 18 the angular fraction is approximately 0.7. Equation 10 shows how to calculate the parameter value t. Note that the angular fraction found when the proxy contact point lies directly on P_1 and P_3 will be either 1 or 0. This guarantees the resulting curve will end at P_1 and P_3 as well as being parallel to L_1 and L_2 at its ends. This allows the resulting curve to join adjacent Bézier curve patches with G^1 continuity.

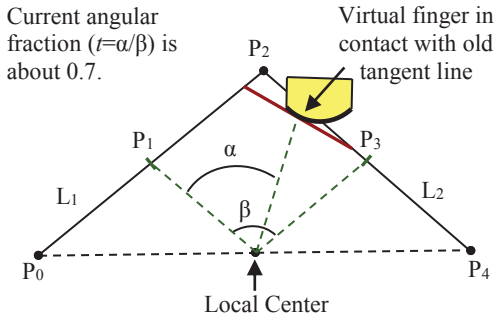

Figure 18. Computing the angular fraction based on the active line segments.

$$t = \frac{\alpha}{\beta} = \frac{\theta_{P1} - \theta_{contact}}{\theta_{P1} - \theta_{P3}} \tag{10}$$

9.4.3 Computing the New Tangent Line

The last step is to compute the new tangent line segment by inputting the computed parametric value t into Equations 9. This tangent line is then used to compute haptic feedback. As the user reaches the midpoint of L_1 or L_2 they also reach the endpoint of the tangent line segment. Thus the tangent line segment should always be extended to eliminate any artifacts that could be felt at this boundary.

CHAPTER 3

HUMAN DETECTION AND DISCRIMINATION OF TACTILE REPEATABILITY, MECHANICAL BACKLASH, AND TEMPORAL DELAY IN A COMBINED TACTILE-KINESTHETIC HAPTIC DISPLAY SYSTEM

Abstract—Many of the devices used in haptics research are over-engineered for the task and are designed with capabilities that go far beyond human perception levels. Designing devices that more closely match the limits of human perception will make them smaller, less expensive, and more useful. However, many device-centric perception thresholds have yet to be evaluated. To this end, three experiments were conducted, using a one degree-of-freedom contact location feedback device in combination with a kinesthetic display, to provide a more explicit set of specifications for similar tactile-kinesthetic haptic devices. The first of these experiments evaluated the ability of humans to repeatedly localize tactile cues across the fingerpad. Subjects could localize cues to within 1.3 mm and showed bias toward the center of the fingerpad. The second experiment evaluated the minimum perceptible difference of backlash at the tactile element. Subjects were able to discriminate device backlash in excess of 0.46 mm on low curvature models and 0.93 mm on high curvature models. The last experiment evaluated the minimum perceptible difference of system delay between user action and device reaction. Subjects were able to discriminate delays in excess of 61 ms. The results from these studies can serve as the maximum (i.e., most demanding) device specifications for most tactile-kinesthetic haptic systems.

1 Introduction

MANY haptic devices used in research applications are over-engineered for their given task. While this provides additional benefits in some fields, it serves as a detriment in the field of haptics. Once a device's performance has exceeded the limits of human perception, any additional precision provides no further benefit, unless directly trying to measure human perception capabilities. Understanding these perceptual limits can provide a more explicit set of specifications for haptic device designs. By closely matching these specifications, haptic devices can become smaller, less expensive, and more useful, expanding their presence as both research and commercial products.

To begin addressing the issue, this paper presents three experiments evaluating perceptual thresholds relating to tactile device design. Each of the following experiments are performed with a tactile device known as a contact location display (CLD), described in detail in Section 3, and the results can serve as the maximum (i.e., most demanding) device specifications for similar tactile-kinesthetic haptic systems. That is, our results apply to systems that provide tactile feedback where the user is experiencing tactile feedback as a function of their limb motions. The first of these three experiments identifies the resolution with which tactile cues can be repeatedly localized on the distal fingerpad. We ask participants to match a touched point on the fingertip by actively adjusting the location of a tactor on the same fingertip. The measured error of this repeated localization procedure provides the maximum positioning error allowed by the tactor in order for two placements of the tactor on the fingertip to be perceived as being at the same position. The second experiment evaluates the minimum perceivable difference in device backlash when positioning a tactile element. Backlash provides both physical cues, through positioning error during motion, and temporal cues, through a delay in the onset of tactor motion after finger motion. As backlash detection is heavily dependent on tactor positioning, the experiment was performed on both a low curvature and a high curvature surface. The results indicate the level of backlash that can be present in a device before it becomes detectable. The third experiment measures the minimum perceivable difference in system delay between user action and device motion. As with backlash, system delay can manifest in both physical and temporal cues. However, the magnitude of these cues is tied with tactor velocity rather than position and thus is often masked by user motion. The detection of system delay was evaluated as a whole and with only the cues provided at the onset of motion. These results provide the maximum amount of system delay that can be present before it becomes noticeable.

The following section provides a brief background concerning the literature most relevant to this research. This is followed by a description of the CLD device and an overview of

- *A.J. Doxon is with the department of Mechanical Engineering, College of Engineering, University of Utah, Salt Lake City, UT 84112. Email: adoxon@gmail.com*
- *D.E. Johnson is with the School of Computing, College of Engineering, University of Utah, Salt Lake City, UT 84112. Email: dejohnso@cs.utah.edu*
- *H.Z. Tanis with the School of Electrical and Computer Engineering, College of Engineering, Purdue University, West Lafayette, IN 47907. Email: hongtan@purdue.edu*
- *W.R. Provancher is with the department of Mechanical Engineering, College of Engineering, University of Utah, Salt Lake City, UT 84112. Email: wil@mech.utah.edu*

the experiments performed. Each of the 3 experiments is then presented in turn, with results and discussion. Finally, results from all experiments are summarized and future work is discussed.

2 Background

2.1 Human Sensing Thresholds

A substantial amount of work has been published regarding the haptic sensing abilities of humans. Biggs & Srinivasan and Hale & Stanney both provide a compilation of some prior work, tabulating their results into an easy-to-use reference [1], [2].

When designing tactile devices, it is important to understand how users judge spatial-tactile information provided to their fingertips. Human ability to localize tactile cues on the fingertip varies as a function of the cue type being given. Textures and micro-bumps, some of the smallest shapes that can be tactilely perceived, are detected through vibrations and skin stretch. Gleeson et al. demonstrated that subjects could detect the direction of skin displacements of 50 μm in the cardinal directions [3]. Loomis and Collins also demonstrated that these skin stretch cues could be detected with a much finer resolution than single-point localization [4]. Loomis also evaluated fingerpad localization with respect to successive single-point tactile cues. Subjects were asked to identify whether the subsequent cue was provided to the right or left of the prior cue. This experiment showed subjects were able to localize cue positions and displacements as fine as 0.17 mm [5]. This localization is different from the two-point limen, which is the minimum separation distance at which 2 simultaneous cues can each be sensed individually. Boven and Johnson report the two-point limen at multiple locations on the body. They report the two-point limen at the fingertip to be around 0.94 mm [6].

An arguably more important threshold to keep in mind when designing tactile devices is that of temporal delay. Many publications have shown that long delays, such as those caused when communicating across networks, can cause significant performance decreases in positioning and manipulation tasks. The vast majority of these studies have investigated the effects of audio and visual delays on performance and perception. Other studies have shown the effects of network delays on kinesthetic haptic interaction [7]. However, relatively little research has been performed with respect to the effect of time delays on user performance in tactile-kinesthetic haptic systems. Of these three domains (audio, visual, and haptic), delays in audio feedback are the most perceptible. Adelstein et al. showed audio delay with respect to a visual image became detectable at around 20 ms [8]. Mania et al. found visual delays with respect to head motion are usually detected around 40 ms but could be detected as low as 30 ms [9]. Jay and Hubbold demonstrated visual delays above 69 ms significantly hindered user performance in a Fitts-type task [10]. In a similar Fitts-type task, Jay and Hubbold also showed that providing delay in haptic feedback is less disruptive than in visual feedback. In this task, the target area was kinesthetically rendered as a solid plane, giving the sensation of striking a solid surface. They found haptic delays in excess of 187 ms to cause a statistically significant performance decrease [10].

While not directly related to a single perception threshold, device backlash should also be considered when designing haptic devices. While most authors agree there should be little-to-no backlash in haptic systems, they rarely report their device's backlash or what an ideal level of backlash should be. Backlash detection can be viewed as a combination of other perception thresholds. Backlash can be sensed as either a small displacement error or as a time delay in device motion based on user velocity. In either case, the resulting minimum detectable backlash is small (likely 100s of micrometers or 10s of milliseconds in scale).

In addition to accounting for tactile perception thresholds, haptic devices should have a bandwidth in excess of their users' and adequate to faithfully render a given virtual environment. Humans are generally estimated to have a maximum bandwidth between 5 and 10 Hz [11]. While user velocity is slower during exploration, tactile device positioning is also affected by changes in surface contours. These relative changes can easily create high frequency tactile cues in excess of 10 Hz. However, very little research has investigated finger velocities during tactile exploration. Generally, tactile devices are designed with high bandwidth to overcome this problem. Frisoli et al. and Lederman & Klatzky discuss the motions and methods of tactile exploration [12], [13], [14]. These motions and methods provide a basic estimate of the relative finger velocities under different exploration conditions.

2.2 Design Guidelines for Tactile Displays

Drewing et al. and Webster et al. discuss some basic guidelines for designing tactile displays [15], [16]. In particular, they place the greatest importance on matching human perception thresholds and miniaturization when designing devices for use in combination with tactile and kinesthetic feedback. Webster et al. also point out that the device's tactor velocities should be capable of exceeding maximum finger exploration velocities. They estimate a safe upper bound for tactor velocities of 30-40 cm/s [15]. The results of both of these studies were applied to their next generation of slip displays.

In related work, Salisbury et al. evaluate the performance of commercially available haptic devices when rendering textures [17]. Their results provide device design guidelines to ensure proper rendering of the vibratory components of textures.

Other publications suggest guidelines for the design of vibrotactile feedback [18], [19] and pin arrays [20], but a number of design parameters for other tactile systems must be gathered from the related psychophysics literature. Little other work discusses design guidelines for building combined tactile and kinesthetic devices.

The results of the present study can be viewed as the most demanding specifications for combined tactile-kinesthetic haptic-feedback systems, including those that display slip (e.g., [21], [22], [15], [16]), tactile pin array (e.g., [22], [23]), contact orientation (e.g., [24], [25], [26]), and contact location [27].

3 Experimental Apparatus

The basic concept of contact location is presented in Fig. 1. Rather than providing all possible tactile information to the user, only the center of contact is rendered through a small tactor. In the current device design, the tactor is only capable of motions in the proximal-distal directions. The contact location display device is mounted to a SensAble Phantom Premium 1.5 through a 3 degree-of-freedom gimbal to allow full motion of the finger. The Phantom provides the kinesthetic force feedback of the system while the contact location display provides tactile feedback.

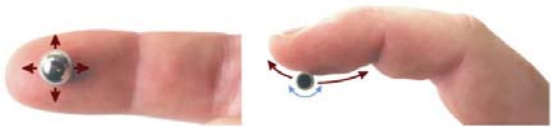

Fig. 1. Concept for contact location feedback. The (left) two-dimensional or (right) one-dimensional center of contact is represented with a single tactile element. The current contact location display is only capable of displaying one-dimensional contacts along the length of the finger (see Fig. 2).

The device utilizes a 1 cm diameter delrin roller as the tactile contact element (tactor). This ensures that only the contact position is provided and no skin stretch is experienced when the contactor is moved along the finger. The position of the roller is controlled via two sheathed push-pull wires attached to a linear actuator mounted on the user's forearm. An open-bottomed thimble is used to securely attach the device to the user's finger. Different sized thimbles can be interchanged onto the CLD to accommodate a wide range of finger sizes. The thimble also provides the anchor points for the push-pull wire sheaths, ensuring the push-pull wires are never in contact with the skin. The roller is held continuously in contact with the fingerpad by two small springs attached to the thimble. Forces are applied to the finger directly through the open-bottomed thimble.

The linear actuator is located on the user's forearm to minimize device inertia at the fingertip and prevent any actuator vibrations from being transmitted to the user's fingertip. While some low magnitude actuator vibrations may be detected by the forearm, the influence of these vibrations is effectively eliminated by the relatively lower sensitivity of the forearm and the user's attention being focused at the fingertip. The user's forearm is supported by a rolling arm rest to allow comfortable positioning of the finger. The linear actuator utilizes a Faulhaber DC Micromotor (1724-024S) with 3.71:1 gearbox and a 3.175 mm pitch leadscrew with an anti-backlash nut to provide approximately 2 cm of linear motion. The device has approximately 0.4 μm of resolution and a bandwidth in excess of 5 Hz. Device backlash at the tactor was characterized to be 0.23 mm throughout its workspace. This backlash is primarily caused by deformations in the push-pull wire sheaths due to friction between the push-pull wires and sheaths. The current device, attached to a Phantom through a 3 degree-of-freedom gimbal, can be seen in Fig. 2. A close up view of the fingertip portion of the device is also shown in Fig. 2.

The device's motor is driven by an AMC 12A8 PWM current amplifier controlled using a Sensoray 626 PCI control card. The device's position is controlled through a PID controller run at 1 kHz. This controller was programmed in

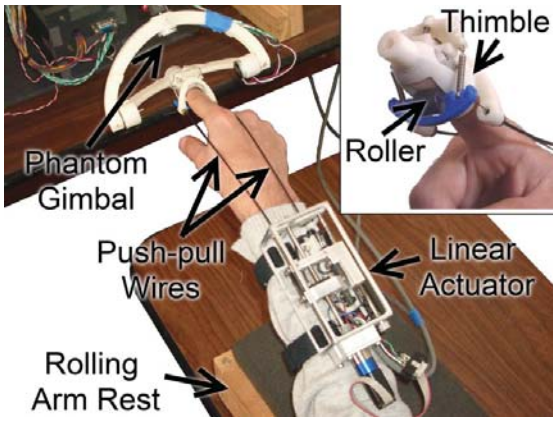

Fig. 2. Contact location display (CLD) attached to a Phantom robot. The user's elbow is supported by a rolling armrest. The user's finger is secured to the CLD via an open bottomed thimble.

C++ and executed in a Windows 7 environment using Windows multimedia timers. Further details about the design and control of this device are related to the earlier version of the device found in [27].

4 General Methods

Three separate experiments were conducted to evaluate perceptual thresholds relating to tactile device design. The results from these experiments can be applied to most tactile-kinesthetic haptic systems. The first of these three experiments identifies the resolution with which users are able to repeatedly localize tactile cues at a given location on their fingerpad. This directly identifies the maximum positioning error a tactile device can have before the error becomes noticeable. The second experiment evaluates the minimum perceivable amount of backlash when positioning a tactile element on the user's fingerpad. Most haptic devices are designed to contain virtually no backlash. Designing closer to the perceptual limit will help relax design tolerances and reduce system costs. Lastly, the third experiment measures the minimum perceivable system delay between user action and device motion. For haptic devices to feel responsive, the whole system delay must be less than the measured value.

During each experiment, the velocities of both the tactor and finger were recorded. These velocities help to identify common interaction speeds when exploring virtual environments. Devices unable to react at these velocities will feel sluggish and unresponsive.

The above experiments are conducted using the contact location display, described in Sect. 3, whose performance exceeds the expected human perceptual limits in all the above cases. One of our goals resulting from these experiments is to miniaturize the design of this tactile display.

Each experiment was performed by the same group of 20 participants (3 female, 3 left handed). Participant ages ranged between 20 and 40. Half of the participants had prior experience using the CLD device.

All three experiments were performed in the same session. A Latin Squares reduction was used to determine experiment order to provide balanced testing. Before each experiment, participants underwent a brief training period to familiarize them with the experiment's task and response process. Each experiment took around 15-20 minutes to complete, with all three experiments taking approximately 1-1.5 hours in total, including breaks. Participants took breaks between experiments and sections within each experiment to reduce fatigue effects.

The participant's arm and testing apparatus were obscured by a cloth cover throughout the duration of each experiment. Experiment instructions were provided on the computer monitor, but no other visual feedback was provided. White noise was played on noise-cancelling headphones during testing to eliminate any auditory cues from device motion. Additional audio cues were provided to assist in pacing the experiment and to indicate transitions between stimuli. The experimental setup can be seen in Fig. 3.

Each of the three experiments utilizes the same base environment. This environment consists of a single 95 mm radius cylinder with its axis of symmetry aligned horizontally from right to left. The cylinder model was chosen to provide an object surface with a constant curvature. The fore-aft motion of the participant's finger along

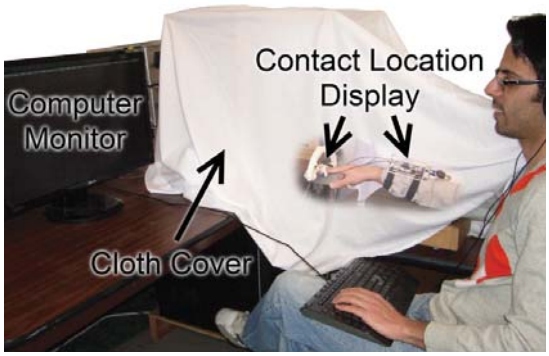

Fig. 3. Experiment setup (cover made transparent for clarity).

the curved surface is natural and comfortable given the kinematics of the CLD as compared to the movement required by a planar surface to achieve the same interaction. The user's virtual finger is represented by a 13 mm sphere, offset such that its surface aligns with the user's fingerpad. Fig. 4 shows a representation of the virtual environment used in the experiments.

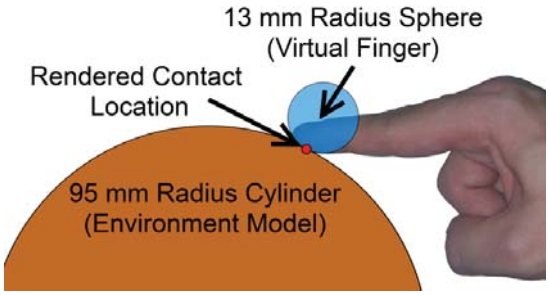

Fig. 4. The virtual environment used in each of the three experiments. This environment was slightly altered in some of the experiments.

5 Repeated Localization of Tactile Cues

The first experiment evaluates the resolution with which users are able to repeatedly locate tactile contact on their fingerpad through a position matching task. This directly identifies the maximum positioning error a tactile device can contain before the error becomes noticeable for sequential contacts. Other studies have clearly shown that even extremely small tactor motions can be detected [28]. Thus, device designs should take into account the expected form of tactor motions during use when determining the amount of acceptable positioning error.

5.1 Methods

Users were instructed to match successive tactile contact locations through interacting with a cylindrical model. The model's position and radius vary but functionally is the same as the base environment described in Section 4.

5.1.1 Procedure

The position matching (repeated localization) task was evaluated at 5 points along the length of the fingerpad (see Fig. 5). These positions are evenly distributed across the workspace of the CLD. The edges of the workspace were avoided as they provide additional references (perceptual anchors) that would artificially increase people's performance at those locations [29]. The spacing between test locations is approximately 2.8 mm.

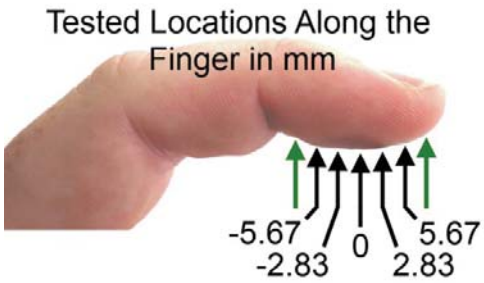

Fig. 5. Five test locations along the length of the fingerpad. Test locations separated by about 2.8 mm. The green arrows denote the edges of the CLD's workspace.

This is larger than the 2 point limen which indicates a different set of mechanoreceptors is being tested with each location [6]. Fig. 5 shows the test locations on the fingerpad, with the labeled points corresponding with those in Figs. 7 and 8. The participants' ability to place the contact was evaluated at each of these 5 locations. Each location was tested 10 times, with the order of the 50 trials randomized for each participant.

Each trial consisted of the following sequence. First, a visual representation of the current tactor position and a target region was shown on the computer monitor (see Fig. 6). The current tactor position is represented by a red sphere. The target region is represented by a green rectangle centered about the chosen test location and spans ±0.25 mm. A participant then moves his/her finger such that the tactor position was within the green rectangle. Once there, the participant was instructed to hold their arm stationary and memorize the position of the tactor on their fingerpad. The participant

Fig. 6. Graphics and instructions displayed to the participant during the experiment. An indicator of tactor position is shown on the left. The red sphere represents the tactor location. The green rectangle represents the target area to proceed. Instructions are shown in the center of the screen.

indicated they were ready to proceed by pressing 'Enter' on the keyboard. A tone would sound and the visual indicator of position was removed, indicating their current position was recorded. The user would then raise their finger above the surface while the radius and position of the cylinder was altered. A second tone would sound to indicate the participant could lower his/her finger onto the new virtual surface. Once on the new surface, the participant moved his/her finger fore/aft such that the tactor's position on his/her fingerpad matched the previously recorded position, to the best of their ability. The participant finished the trial by pressing 'Enter' again to record his/her current "matched" position. The visual indicator of position was displayed again and the next trial would begin.

5.1.2 Stimuli

The environment model is a horizontal cylinder similar to the base environment described by Fig. 4 in Section 4. Between each matching task the position and radius of the virtual model was randomly selected to limit the effect of curvature, proprioceptive, and kinesthetic cues. The cylinder's radius could vary between 50 mm and 140 mm (mean 95 mm). The fore-aft position of the cylinder was chosen such that users were required to move the CLD's tactile element at least 4 mm to match its previous position and that a portion of the cylinder would always lie directly below the user's finger. This resulted in the center of the cylinder shifting back and forth by no more than 50 mm from its starting position over the course of the experiment. The position and radius were also chosen such that the full range of motion of the CLD lays within the workspace of the Phantom force feedback device.

5.2 Position Matching Results and Discussion

No effects of testing order or prior experience were observed. The positioning error was evaluated in 2 ways, the signed error and the absolute error. While positive and negative errors may cancel each other in the average signed error, the absolute error, which is the absolute value of the signed error, is a more stringent measure of the accuracy with which participants could position the tactor.

The mean absolute-error during tactile cue localization for all test locations is approximately 1.3 mm. The mean absolute-errors were not found to be statistically different among the 5 test locations [$F(4,995)=0.5$, $p=0.733$]. This lack of difference indicates that tactile cue localization does not vary with location on the fingerpad. Fig. 7 shows the mean absolute-errors and their 95% confidence intervals for each of the 5 test locations across all participants. Hence, in order to avoid detection of tactile element positioning errors, these errors must be kept less than 1.3 mm. This maximum error is measured for sequential contact of the tactile element. Much smaller tactor motions can be detected when they are experienced instantaneously [28]. Thus devices require significantly higher position resolution to provide smooth interaction than for detecting position error for sequential contacts. Therefore, even though [28] suggests that a tactile device will require high positioning resolution, the above results imply that a device may have significant position error (i.e., 1.3 mm) after large motions or sequential contact where the user is more likely to lose their immediate reference.

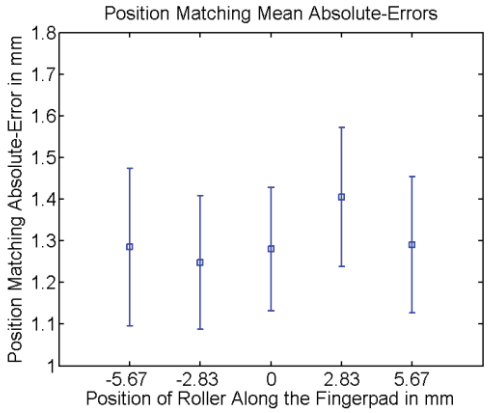

Fig. 7. Mean absolute-error and its 95% confidence intervals among the 5 test locations across all participants.

The mean localization error, in contrast to the mean absolute-error, provides another interesting insight into tactile localization. The mean errors are statistically different with respect to test location [$F(4,995)=18.92$, $p<0.001$] (see Fig. 8). These differences indicate a linear response bias toward the center of the fingerpad. This bias is relatively small compared to the mean absolute-error. Fig. 8 shows the mean localization errors and their 95% confidence intervals for each of the 5 test locations across all participants. The error at each test location strongly fits a normal distribution and contains little skew. The normal distribution may also indicate that this bias toward the center of the fingerpad is not likely device related in origin. One possible explanation for this bias is that users naturally orient their fingerpad normal to any surface they are

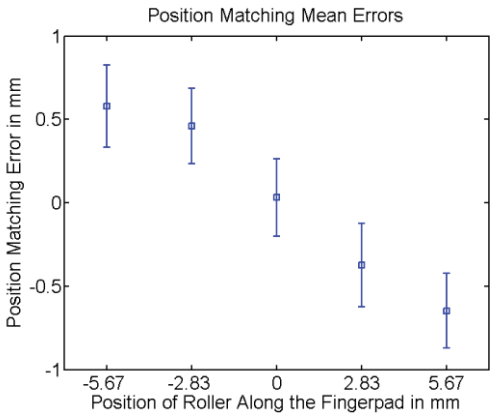

Fig. 8. Mean localization error and its 95% confidence intervals among the 5 test locations across all participants.

exploring. Doing so positions the CLD's tactor closer to the center of the fingerpad. Participants may have subconsciously adjusted their finger during matching, thus providing a bias toward the center of the fingerpad. Interaction forces with the surface remain relatively constant between trials with forces varying around 1-2 N depending on the participant. Force levels did not change as a function of position and thus are not a likely cause of this error.

6 Discrimination of Tactor Backlash

The following experiment examines participants' ability to discriminate between the CLD's inherent backlash and an artificially-increased backlash. The CLD's inherent backlash is 0.23 mm and it is not noticeable by the experimenters under typical conditions the CLD system is used. Since the CLD's minimum backlash is non-zero, we treat the experimental task as a discrimination, not a detection, task. However, for all practical purposes, the discrimination thresholds reported here can be viewed as approaching the detection thresholds for backlash under similar conditions.

The discrimination task was performed through a paired-comparison (two interval), forced-choice paradigm. Backlash perception is presumably done through a combination of haptic and temporal sensing. Identifying this perceptual limit will allow tactile-kinesthetic devices to potentially include more system backlash, reducing their cost and complexity, while maintaining the imperceptibility of backlash.

Because the effects of backlash are depended on the positioning of the tactile element the threshold was evaluated on low and high curvature surfaces as two separate halves of the experiment. This is especially important as the curvature of the surface directly affects the positioning of the tactor for devices utilizing contact location. Fig. 9 shows the finger motion required to produce the same tactor displacement for low and high curvature models. On high curvature models, such as at an edge formed by two faces, the rendered contact location remains stationary on the model (and in the world) as a user moves his/her finger. Thus the CLD's tactor will move at the same rate as the user's finger in the opposite direction. On low curvature models the contact location moves along the surface with the finger, slowing tactor motion with respect to finger motion. This means participants must move their finger farther before the tactor is driven enough to overcome the CLD's backlash and begin moving, thus magnifying the deadband created by the backlash and making it easier to detect.

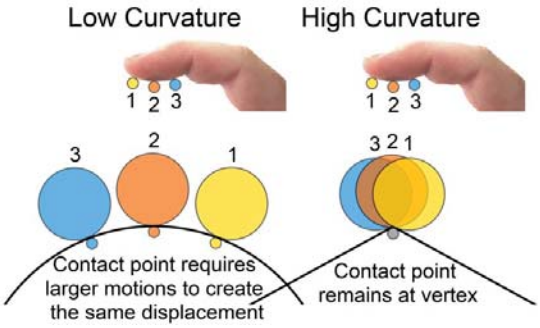

Fig. 9. Contact location positioning on high and low curvature surfaces as the finger is moved horizontally left and right. The finger must move farther on low curvature surfaces to create the same tactor displacement as shown on the high curvature surface.

6.1 Methods

6.1.1 Procedure

This experiment utilized a paired-comparison (two interval), forced-choice paradigm, with a 1-up, 2-down adaptive procedure [30]. During each trial the participant was presented with two intervals: a reference interval without added backlash, and a comparison interval with added virtual backlash. The order of the reference and comparison intervals was randomized. Participants were instructed to indicate which of the two intervals contained more backlash. The amount of added backlash increased with each incorrect response and decreased after two consecutive correct responses. The threshold

obtained corresponded to the 70.7% confidence interval on the psychometric function [30].

Each trial was conducted as follows. First, the participant interacts under the first interval. Once s/he has a feel for the first interval s/he raises the finger and presses 'Enter'. Two tones sound to let the participant know the second interval is now active. After lowering his/her finger into contact with and interacting with the virtual surface under the second interval the participant raises the finger and presses either '1' to indicate the first interval contained more backlash, or '2' to indicate the second interval contained more backlash. A single tone sounds, alerting the participant that a new interval 1 is now ready and the next trial is ready to commence.

The experiment continues until the participant has finished 14 reversals. A reversal occurs when the added virtual backlash increases after a decrease, or vice versa. A large step size (0.3 mm) was used for the first 4 reversals to provide faster initial convergence. A reduced step size (0.06 mm) was used for the remaining 10 reversals to provide better accuracy in determining the discrimination threshold. The step sizes for each stage and model were chosen during pilot testing and fixed for all participants.

6.1.2 Stimuli

The computed tactor position was augmented with a virtual backlash to emulate larger device backlash levels. Each pair of compared backlash intervals consisted of a virtual model rendered without any added virtual backlash and a model rendered with some small amount of added virtual backlash.

The experiment was split into two halves to evaluate the discriminability of backlash on low and high curvature virtual models. In one half of the experiment, participants interacted with the top edge of a horizontally extruded isosceles triangle with a 2 degree angle between its nearly vertical faces. During the other half of the experiment, participants interacted with the base environment's cylinder model (95 mm radius cylinder). In this case, the ratio between the virtual finger radius and the cylinder radius magnifies the effect of the backlash by approximately 7.3:1 (when the participant maintains a horizontal finger orientation). Half of the participants experienced the low curvature model first, while the other half experienced the high curvature model first.

6.2 Backlash Results and Discussion

No effects of testing order or prior experience were observed. The minimum added virtual backlash when tested with both low and high curvature virtual models was statistically different from 0 [low curvature: $t(19)=5.18$, $p<0.001$; high curvature: $t(19)=7.34$, $p<0.001$]. After the experiment, most participants reported that their method for detecting backlash involved making a small finger movement and attempting to detect the presence (or the lack) of a corresponding motion of the tactor. This indicates that the haptic portion of the cue is the dominant factor when detecting backlash. This is further supported by the larger positioning errors found in the system delay experiment (Section 7).

The backlash discrimination threshold when interacting with the low curvature model was approximately 0.46 mm. The backlash discrimination threshold on the high curvature model was 0.93 mm (see Fig. 10). As expected, there is a statistically significant decrease in the threshold when interacting with lower curvatures [$F(1,38)=9.38$, $p=0.002$] due to the magnified backlash deadband as explained at the beginning of Section 6. Fig. 10 shows the means and 95% confidence intervals of the backlash thresholds for both the low and high curvatures. The backlash discrimination threshold is expected to decrease further as curvature decreases. However, at some point the effects of low curvature will slow the tactor motion to an imperceptible degree and backlash can no longer be detected.

As mentioned earlier, the CLD's inherent backlash of 0.23 mm is not noticeable by the experimenters. Assuming that 0.23 mm is indeed

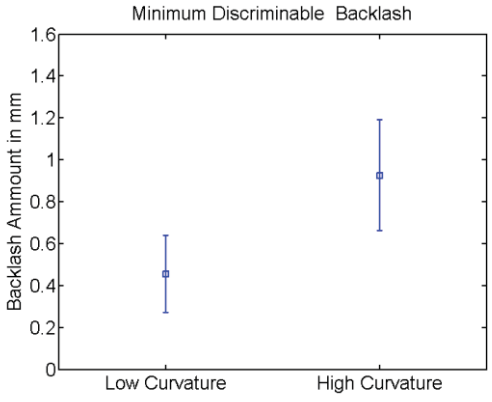

Fig. 10. Minimum discriminable backlash means and their 95% confidence intervals for low and high curvature models.

below the human backlash detection threshold (which requires a no-backlash system to confirm, which is beyond the scope of the present study), our results can also be interpreted as detection thresholds by adding 0.23 mm to the backlash discrimination thresholds to compute the total system backlash. We would then conclude that the backlash detection thresholds for low and high curvature models are approximately 0.69 mm and 1.16 mm, respectively.

The above backlash perception thresholds were evaluated while participants were specifically looking for backlash. Under general use, participants will not be devoting their full attention to detecting backlash, thus larger device backlashes on lower curvature models may go unnoticed.

7 Discrimination of System Delay

The following experiment examines participants' ability to discriminate between the CLD's inherent system delay and an artificially-increased delay. The system delay is defined as the time difference between user action and device reaction. The CLD's inherent delay is around 1-2 ms and not noticeable under typical uses. Strictly speaking, our experiment should be treated as a discrimination task between a non-zero inherent system delay and a delay with additional virtual delay. However, for all practical purposes, the delay discrimination thresholds reported here can be viewed as approaching the delay detection thresholds under similar conditions.

The discrimination task was performed through a paired-comparison (two interval), forced-choice paradigm. More system delays will lead to more disassociation between tactile and kinesthetic cues or more sluggish reactions from the system. System delay manifests itself in three forms during a single motion. First, there is a delay in tactor motion after the user's finger has begun moving ("front-end" delay). This delay can be masked by the user's own kinesthetic motion. Second, there is a position error during motion. However, for small system delays this error is too small to be detectable. Lastly, after the user's finger has stopped motion, the tactor will continue its motion for a time ("back-end" delay). This cue, after the participant has stopped moving, is expected to be the most salient as there is no haptic masking of the tactor motion, and the remaining tactor motion can easily be measured temporally.

Perception of the delay was evaluated in two ways to understand the dominant cues in its detection. First, discrimination of system delay was measured as a whole. Second, only the "front-end" component of delay was evaluated.

7.1 Methods

7.1.1 Procedure

As with the backlash discrimination experiment in Section 6, this experiment utilized a paired-comparison (two interval), forced-choice paradigm, with a 1-up, 2-down adaptive procedure [30]. During each trial, the participant was presented with two intervals: a reference interval without added delay, and a comparison interval with added virtual system delay. The order of the reference and comparison intervals presented was randomized. Participants were instructed to indicate which of the two intervals contained more system delay. The amount of added delay increased with each incorrect response and decreased after two consecutive correct responses. The threshold obtained corresponded to the 70.7% confidence interval on the psychometric function [30].

Each trial was conducted as follows. First, the participant interacts with the first interval. Once they have a feel for that interval they raise their finger and press 'Enter'. Two tones sound to let the participant know the second interval is now available. After interacting with the second interval, the participant raises his/her finger and presses either '1,' to indicate the first surface contained more system delay, or '2,' to indicate the second surface contained more system delay. A single tone then sounds, alerting the participant that a new interval '1' is in place and the next trial can begin.

The experiment continues until the participant has completed 14 reversals. A reversal occurs when the additional virtual system delay increases after a decrease, or vice versa. A large step size (15 ms) was used for the first 4 reversals to provide faster initial convergence. A reduced step size (6 ms) was used for the remaining 10 reversals to provide better accuracy in determining the discrimination threshold. The step sizes for each stage and section were chosen during pilot testing and fixed for all participants.

7.1.2 Stimuli

Artificial system delay is created by passing the desired tactor position through a FIFO buffer. The length of the FIFO buffer determines the number of haptic cycles the command is delayed. The haptic loop is run at 1 kHz such that each cell

in the FIFO buffer delays the signal by 1 ms. As in the backlash discrimination experiment, each set of paired comparisons consists of a model rendered with this additional virtual delay and a model rendered without any virtual delay.

This experiment was split into two halves. Both halves were conducted using the base environment (95 mm radius cylinder). Pilot testing indicated that curvature had little effect on discrimination of system delay. This is likely due to the fact that the participants could simply move faster to increase the effect of the delay and overcome the slowing effect of low curvature on the tactor motion. During the first half of the experiment, discrimination of whole system delay was evaluated. Participants were allowed to freely interact with the cylinder as desired. During the second half of the experiment only the "front-end" delay was evaluated. The continued tactor motion after the participant stopped finger movement was removed by restricting user interaction with the model. In this case participants would contact the surface on one side then sweep their finger to the other. When the tactor reached approximately two-thirds of the way across its workspace, it would freeze while the participant continued motion, thus eliminating any end of motion cues. The participant would then raise their finger and lower it back onto the surface to unfreeze the tactor and repeat the process.

7.2 Delay Discrimination Results and Discussion

No effects of testing order or prior experience were observed. The discrimination threshold of system delay was found to be approximately 61 ms. However, when only evaluating the "front-end" delay, the threshold was 132 ms (see Fig. 11). As expected, the "front-end" delay is significantly less noticeable than the system delay as a whole [$F(1,38)=49.89$, $p<0.001$]. This implies that the tactile motion that occurs after the finger has stopped moving is likely the dominant cue when detecting system delay as a whole. The larger threshold of the "front-end" delay can be partially attributed to the restrictions placed on participant's finger motion during that portion of the experiment. However, the majority of the difference can still be attributed to the participant's finger motion masking the delay in tactor motion. Fig. 11 shows the means and 95% confidence intervals of the system delay thresholds for both the whole system delay and the "front-end" delay.

The positioning error at the thresholds is larger than the backlash detection threshold. The average position error created by the whole system lag is 0.94 mm. This is about twice the backlash threshold on the low curvature object. Velocities in the "front-end" delay portion were comparable thus resulting in a much larger error. This further supports the argument that the finger motion masks errors in tactor positioning.

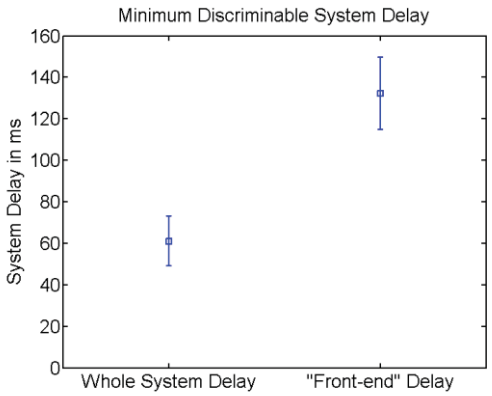

Fig. 11. Mean values for the discrimination thresholds of system delay and their 95% confidence intervals for whole system delay and "front-end" delay.

The CLD's inherent delay of 1-2 ms is negligible in comparison to the 61 ms and 132 ms discrimination threshold for the whole delay and the "front-end" delay. Assuming that 1-2 ms is below the human delay detection threshold (which requires a no-delay system to confirm, which is beyond the scope of the present study), our discrimination thresholds can also be interpreted as detection thresholds by adding the 1-2 ms to the delay discrimination thresholds. Numerically, it does not make much difference whether the 1-2 ms is added to the discrimination thresholds to obtain the corresponding detection thresholds for the whole and "front-end" delays.

The system delay measured here represents the settling time of the system as a whole and can be used to improve devices in a variety of ways. This delay can take the form of larger device inertia or a slower settling controller with lower gains for improved stability. As with the backlash perception experiment in Section 6, participants will not be actively looking for system delay during most uses, thus larger system delays may go unnoticed.

8 Velocity Data

During each of the 3 presented experiments the position and velocity of the participant's finger and the device's tactor was captured. This data

provides valuable insights into common interaction speeds when exploring simple virtual environments. Velocities from the "front-end" delay experimental task are not included in this analysis as participant motion was restricted and does not represent natural participant interaction. These velocities were similar in magnitude to those in the unrestricted whole system delay case.

Average finger velocity during exploration of low curvature surfaces varied between 32 mm/s for precision motions to 74 mm/s during fast motions. Tactor velocities are significantly lower than finger velocities in the majority of the experiment due to the slowing effect of low curvature surfaces. Tactor velocities ranged between 5 mm/s for precision tasks and 19 mm/s during the high curvature backlash task where tactor speed was equal to finger speeds (when a single finger orientation is maintained). The reported velocities on low curvature objects indicate a ratio between tactor and finger velocity closer to 5:1 as opposed to the expected 7.3:1 ratio between the finger model and object model. However, the collected position and orientation data shows participants rolling their fingers as they explored the low curvature surfaces. The 7.3:1 ratio is only true if no orientation changes occur during motion. Figs. 12 and 13 show the mean and 95% confidence intervals of recorded tactor and finger velocities for all participants under each experimental condition.

These recorded velocities provide insight into the necessary responsiveness of tactile devices. Such devices should be capable of tactor motions in excess of 20 mm/s, though the majority of tactile exploration on low curvature models appears to occur below 10 mm/s. Ideally, tactile devices should be capable of velocities exceeding maximum finger exploration (near 70 mm/s) as tactor velocities match finger velocities on high curvature surfaces. While finger and desired tactor velocities can exceed 200 mm/s it is unlikely that users will be able to actively discern surface features at those speeds, thus making this high velocity an unnecessary design requirement.

9 Summary and Future Work

Three experiments were run to evaluate factors relevant to tactile display device design. The first of these experiments identifies the resolution with which the user is able to repeatedly place a contact at a given location on the fingerpad. Participants are able to localize tactile cues to within 1.3 mm on their fingerpad. Cue localization is biased toward the center of the fingerpad. These results stipulate the maximum positioning error the device should achieve after large or sequential motion.

The second experiment evaluates the minimum perceivable difference in backlash in positioning a tactile element. Subjects were able to discriminate device backlash in excess of 0.46 mm on low curvature models and 0.93 mm on high curvature models. Since the device's inherent backlash (0.23 mm) is most likely below human detection threshold, the discrimination results are interpreted as backlash detection thresholds when the device's inherent backlash is taken into account. Accordingly, backlash becomes detectable at levels as low as 0.69 mm on low curvature models. High curvature models make backlash detection more difficult, increasing the threshold to 1.16 mm. The haptic

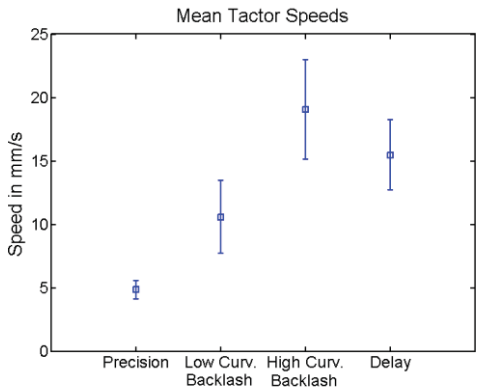

Fig. 12. Tactor velocity mean and 95% confidence intervals during each experimental condition. Front delay not evaluated as participant motions were restricted.

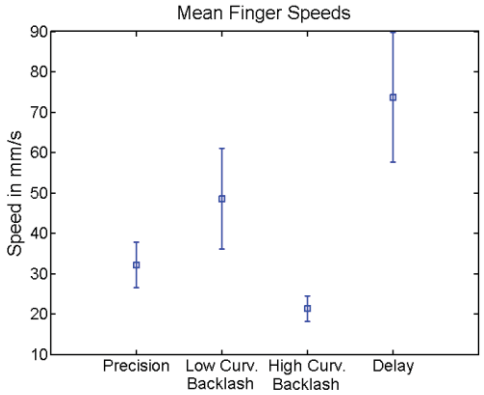

Fig. 13. Finger velocity mean and 95% confidence intervals during each experimental condition. Front delay not evaluated as participant motions were restricted.

portion of backlash was found to be the dominant cue used in detection. In contrast to the first experiment these thresholds indicate the positioning requirements for small or immediate motions.

The third experiment measures the minimum perceivable difference in system delay between user action and device motion. Since the CLD's inherent delay (1-2 ms) is negligible, the discrimination results can be interpreted as delay detection thresholds. Therefore, system delay on tactile output can be as large as 61 ms before it can be detected. The back-end delay (tactile motion after user motion has ceased) was the dominant cue of system delay. Front-end delay is masked by finger motion and was found to become detectable at around 132 ms. The position error at the thresholds was found to be larger than the detection threshold for backlash on the same model, further indicating the masking effects of motion and the dominance of the haptic portion of backlash cues when detecting the threshold. These results determine the allowable system delay before it is noticeable.

During each experiment, the velocities of both the tactor and finger were recorded. Subjects explored low curvature models with finger velocities ranging from 32 mm/s for precision motions to 74 mm/s during fast motions. Tactor velocities are significantly lower than finger velocities in the majority of the experiment due to the slowing effect of low curvature surfaces (see Section 6). As such, devices should be capable of tactor velocities in excess of 20 mm/s, but ideally be able to exceed the 74 mm/s finger velocity found during rapid exploration.

The above evaluated perceptual limits provide the foundation needed to design smaller, less expensive, and more capable tactile devices, expanding their presence as both research and commercial products, while creating perceptibly identical devices.

Future work will involve designing a more compact 2 degree-of-freedom contact location display based on the above guidelines. Use of this new device is aimed at providing more insight into tactile interaction in multifinger manipulation.

10 Acknowledgments

This work was supported, in part, by the National Science Foundation under awards IIS-0904456 and IIS-0904423.

11 References

[1] S. Biggs and M. Srinivasan (2002). Haptic interfaces. In Handbook of virtual environments, pp. 93-116, 2002.

[2] K. Hale and K. Stanney (2004). Deriving haptic design guidelines from human physiological, psychophysical, and neurological foundations. In IEEE conference on Computer Graphics and Applications, vol 24(2), pp. 33-39, 2004.

[3] B. Gleeson, S. Horschel, and W. Provancher (2010). Perception of Direction for Applied Tangential Skin Displacement: Effects of Speed, Displacement and Repetition. IEEE Transactions on Haptics - World Haptics Spotlight, Vol. 3(3), pp. 177–188, 2010.

[4] J. Loomis and C. Collins (1978). Sensitivity to shifts of a point stimulus: An instance of tactile hyperacuity. In Attention, Perception, & Psychophysics, vol 24(6), pp. 487-492, 1978.

[5] J. Loomis (1979). An Investigation of Tactile Hyperacuity. In Sensory Processes, vol 3, pp. 289-302, 1979.

[6] R. Boven and K. Johnson (1994). The limit of tactile spatial resolution in humans: Grating orientation discrimination at the lip, tongue, and finger. In Neurology, vol 44(12), pp. 2361-2361, 1994.

[7] T. B. Sheridan and W. R. Ferrell. Remote manipulative control with transmission delay. IEEE Transactions on Human Factors in Electronics, vol. 1, pp. 25-29, 1963.

[8] B. Adelstein, D. Begault, M. Anderson, E. Wenzel (2003). Sensitivity to haptic-audio asynchrony. In Proceedings of the 5th international conference on Multimodal interfaces. ACM, 2003.

[9] K. Mania, B. Adelstein, S. Ellis, M. Hill (2004). Perceptual sensitivity to head tracking latency in virtual environments with varying degrees of scene complexity. In Proceedings of the 1st Symposium on Applied perception in graphics and visualization. ACM, 2004.

[10] C. Jay and R. Hubbold (2005). Delayed visual and haptic feedback in a reciprocal tapping task. In proceedings of the first joint IEEE Eurohaptics Conference 2005, Symposium on Haptic Interfaces for Virtual Environment and Teleoperator Systems 2005, World Haptics 2005, 2005.

[11] T. Brooks (1990). Telerobotic response requirements. In Proceedings of IEEE International Conference on Systems, Man and Cybernetics, 1990.

[12] A. Frisoli, M. Bergamasco, S. Wu, and E. Ruffaldi (2005). Evaluation of multipoint contact interfaces in haptic perception of shapes. Multi-point interaction with real and virtual objects. Springer Tracts in Advanced Robotics, vol 18, pp. 177–188, 2005.

[13] S. Lederman and R. Klatzky (1987). Hand movements: A window into haptic object recognition. In Cognitive psychology, vol 19(3), pp. 342-368, 1987.

[14] S. Lederman and R. Klatzky (1993). Extracting object properties through haptic exploration. In Acta psychologica, vol 84(1), pp. 29-40, 1993.

[15] R. J. Webster III, T. E. Murphy, L. N. Verner, and A. M. Okamura. A novel two-dimensional tactile slip display: design, kinematics and perceptual experiments. In ACM Transactions on Applied Perception (TAP), vol. 2(2), pp. 150-165, 2005.

[16] K. Drewing, M. Fritschi, R. Zopf, M. O. Ernst, and M. Buss. First evaluation of a novel tactile display exerting shear force via lateral displacement. In ACM Transactions on Applied Perception (TAP), vol. 2(2), pp. 118-131, 2005.

[17] C. Salisbury, B. Gillespie, H. Tan, F. Barbagli, and K. Salisbury. What you can't feel won't hurt you: Evaluating haptic hardware using a haptic sensitivity contrast function. In IEEE Transactions on Haptics, vol. 4(2), pp. 134-146, 2011.

[18] L. A. Jones and N. B. Sarter. Tactile displays: Guidance for their design and application. In Human Factors: The

Journal of the Human Factors and Ergonomics Society, vol. 50(1), pp. 90-111, 2008.
[19] K. S. Hale and K. M. Stanney. Deriving haptic design guidelines from human physiological, psychophysical, and neurological foundations. In Computer Graphics and Applications, IEEE, vol. 24(2), pp. 33-39, 2004.
[20] G. Moy, U. Singh, E. Tan, and R. S. Fearing. Human Psychophysics for Teletaction System Design. In Haptics-e, vol. 1(3), pp. 1-20, 2000.
[21] M. Salada, J. Colgate, P. Vishton, and E. Frankel. An experiment on tracking surface features with the sensation of slip. WHC 2005. First Joint EuroHaptics Conference and Symposium on Haptic Interfaces for Virtual Environment and Teleoperator Systems, 2005, pp. 132-137, 2005.
[22] M. Fritschi, M. Ernst, and M. Buss. Integration of kinesthetic and tactile display – a modular design concept. In 2006 EuroHaptics Conference, 2006.
[23] I. Sarakoglou, N. Garcia-Hernandez, N. Tsagarakis, and D. Caldwell. A high performance tactile feedback display and its integration in teleoperation. IEEE Transactions on Haptics, vol. 5, no. 3. pp. 252-263, 2012.
[24] A. Frisoli, M. Solazzi, F. Salsedo, and M. Bergamasco. A fingertip haptic display for improving curvature discrimination. Presence: Teleoperators and Virtual Environments, vol. 17, no. 6, pp. 550-561, Oct. 2008.
[25] H. Dostmohamed and V. Hayward. Trajectory of contact region on the fingerpad gives the illusion of haptic shape. Experimental Brain Research, vol. 164, no. 3, pp. 387-94, July, 2005.
[26] F. Chinello, M. Malvezzi, C. Pacchierotti, and D. Prattichizzo. A three DoFs wearable tactile display for exploration and manipulation of virtual objects. In Proceedings of IEEE, Haptics Symposium (HAPTICS), pp. 71-76, 2012.
[27] W. R. Provancher, M. R. Cutkosky, K. J. Kuchenbecker, and G. Niemeyer (2005). Contact location display for haptic perception of curvature and object motion. International Journal of Robotics Research, vol 24(9), pp. 691–702, 2005.
[28] A. J. Doxon, D. E. Johnson, H. Z. Tan, and W. R. Provancher. Force and contact location shading methods for use within two-and three-dimensional polygonal environments. Presence: Teleoperators and Virtual Environments, vol. 20(6), pp. 505-528, 2011.
[29] N. I. Durlach, L. A. Delhorne, A. Wong, W. Y. Ko, W. M. Rabinowitz, and J. Hollerbach. Manual discrimination and identification of length by the finger-span method. Perception & Psychophysics, vol 46(1), pp. 29-38, 1989.
[30] H. Levitt, Transformed up-down methods in psychoacoustics. In Journal of the Acoustical Society of America, vol. 49, pp. 467-477, 1971.

Andrew J. Doxon earned a B.S. in Electrical Engineering at the New Mexico Institute of Mining and Technology in 2008 and an M.S. in Electrical and Computer Engineering at the University of Utah in 2010. He is currently pursuing a Ph.D. in Mechanical Engineering at the University of Utah. His primary research focuses on improving combined tactile and kinesthetic haptic devices, by improving the design of new tactile devices and the algorithms that drive them.

David E. Johnson is a research scientist at the University of Utah's School of Computing. He earned a B.A. in Computer Science and Physics at Carleton College and his Ph.D. in Computer Science at the University of Utah, focusing on geometric computations for haptic rendering. His current interests are in applying geometric computations to the area of robotics.

Hong Z. Tan received her Bachelor's degree in Biomedical Engineering (in 1986) from Shanghai Jiao Tong University and earned her Master and Doctorate degrees (in 1988 and 1996, respectively), both in Electrical Engineering and Computer Science, from the Massachusetts Institute of Technology (MIT). She was a Research Scientist at the MIT Media Lab from 1996 to 1998 before joining the faculty at Purdue University. She is currently a professor of electrical and computer engineering, with courtesy appointments in the school of mechanical engineering and the department of psychological sciences. Tan founded and directs the Haptic Interface Research Laboratory at Purdue University. She is currently editor-in-chief of the World Haptics Conference editorial board. Tan served as the founding chair of the IEEE Technical Committee on Haptics from 2006-2008. She was a recipient of the National Science Foundation CAREER award from 2000-2004. Her research focuses on haptic human-machine interfaces in the areas of haptic perception, rendering and multimodal performance. She is a senior member of the IEEE.

William R. Provancher earned a B.S. in Mechanical Engineering and an M.S. in Materials Science and Engineering, both from the University of Michigan. His Ph.D. from the Department of Mechanical Engineering at Stanford University was in the area of haptics, tactile sensing and feedback. His postdoctoral research involved the design of bio-inspired climbing robots. He is currently a tenured Associate Professor in the Department of Mechanical Engineering at the University of Utah. He teaches courses in the areas of mechanical design,

mechatronics, and haptics. His active areas of research include haptics and tactile feedback. Dr. Provancher is an Associate Editor of the IEEE Transactions on Haptics and Co-Chair of the Technical Committee on Haptics. He received an NSF CAREER award in 2008 and has won Best Paper and Poster Awards at the 2009 and 2011 World Haptics Conferences for his work on tactile feedback.

CHAPTER 4

2-DOF CONTACT LOCATION DISPLAY FOR USE IN MULTIFINGER MANIPULATION

4.1 Introduction

As virtual environment interfaces advance, direct manipulation of objects in those environments becomes more common. The most realistic interfaces allow multifinger dexterous interaction. Providing kinesthetic feedback (i.e., force feedback) to give the virtual objects a sense of presence makes these interfaces more intuitive. However, due to the limited feedback that can be provided kinesthetically, these haptic interfaces can still be difficult to use efficiently. The more realistic the interactions become, the more difficult it becomes to pickup and accurately manipulate virtual objects. Just as it is difficult to manipulate objects with numb fingers, a lack of tactile feedback limits user performance. Providing tactile feedback in addition to kinesthetic feedback can enhance usability and improve user interaction during multifinger manipulation [1], [2], [3]. This paper investigates the effects of providing contact-location feedback during multifinger manipulation through a contact-location display (CLD) device [4]. Prior studies with the CLD have investigated its effects on identification and single-finger manipulation [5], [6]. However, in these studies, the CLD was either only capable of providing feedback along a single degree-of-freedom (DOF) [5], or contained significant backlash and a limited workspace [6]. These previous designs are not well suited to be used in a

multifinger setup due to size and actuator limitations.

To begin addressing the effects of providing contact location in multifinger manipulation tasks, we have developed a new CLD device and performed two simple experiments with it. This new device is smaller, weighs less, and provides a full 2-DOF workspace that covers the bottom hemisphere of the finger. The device is described in detail in Section 3. This paper's experiments evaluate the device, and explore the effects of providing contact location on two separate aspects of manipulation: picking up an object and reorientation of an object. The first experiment requires participants to pick up a series of spheres under different rendered friction levels. The second experiment requires participants to reorient a flat surface on a cylindrical object with respect to a fixed reference orientation.

The following section provides a brief background concerning manipulation research and combined tactile kinesthetic feedback devices. We then present the design and characterization of our new 2-DOF CLD device. This is followed by the procedure, results, and discussion of the two experiments which evaluate the effects of contact location feedback on multifinger manipulation. Finally, results from both experiments are summarized and future work is discussed.

4.2 Background

The following sections provide a background on multifinger manipulation and combined tactile kinesthetic devices.

4.2.1 Multifinger Manipulation

Below is a short summary of research involving multifinger manipulation. Frisoli et al. conducted multifinger shape recognition experiments using kinesthetic feedback with one, two, and three fingers [7]. In contrast to identification with bare fingers on real objects, Frisoli et al. found that the number of contact points did not improve subject identification. They attribute this lack of improvement to subjects repeatedly losing contact with the object during exploration [7]. In a later study, Frisoli et al. state this lack of improvement is due to a lack of physical contact location and geometric information on orientation, curvature, contact area, and friction [2].

In a similar vein of studies, Jansson and Monaci investigated shape recognition of real objects where subjects' fingers were either covered by a hard sheath (removing tactile information) or touching the object directly [8]. Jansson and Monaci demonstrated that without tactile information, multiple contact points do not improve performance. They suggest that adding "spatially distributed" contact information to each contact area will not only improve performance, but also cause increasing the number of fingers contacting the surface to improve results.

King et al. evaluated the perceptual thresholds for single- vs. multifinger haptic interactions [9]. They evaluated the minimum detectable force applied to one or more fingers. Their results indicate that force detection is independent of the number of fingers that the force is applied to, i.e., using more fingers does not improve perception of small forces.

McKnight et al. investigated the contribution of haptic feedback in multifinger manipulation when vision is present [10]. Their research shows that the addition of haptic

information allows users to more accurately position and orient virtual objects, but also slightly increases the overall time taken to complete the task.

Kohno et al. developed a multifinger kinesthetic display that provides haptic interactions to up to four fingers on each hand [11]. They evaluated the differences in time to align dots on two spheres with two, three, and four fingers on each hand. The spheres were presented to participants under four conditions: bare fingers manipulating real spheres, capped fingers (no tactile information) manipulating real spheres, haptically rendered spheres, and pure visual feedback. They found the addition of more fingers allowed subjects to more easily manipulate the spheres in all cases. They also show no differences in completion time between capped fingers and haptically rendered spheres.

In addition to perception research, there are several articles developing algorithms for haptic rendering of multicontact interactions. Harwin and Melder have developed a friction cone-based method to be used with god-object rendering algorithms [12], [13]. Otaduy and Lin have demonstrated an algorithm using implicit integration to render six degree-of-freedom interactions between two haptic models [14].

4.2.2 Combined Tactile and Kinesthetic Feedback Devices

Below is a short summary of tactile devices that have been designed for use in combination with kinesthetic feedback. Many of these devices cannot be used in a multifinger setup due to size or space restrictions, and instead are used with a single finger to provide combined tactile and kinesthetic interactions.

Salada et al. conducted several studies investigating the effects of slip or sliding feedback in combination with kinesthetic motions [15]. His device utilized a rotating wheel to provide slip and sliding feedback to the user's fingerpad. Since then, others have

developed slip displays and integrated them with kinesthetic force feedback devices [16], [17], [18]. However, because these slip displays tend to be large and cumbersome, they cannot be utilized in multifinger setups that allow users to grasp objects.

Fritschi et al. investigated providing tactile feedback though a pin array in combination with kinesthetic feedback [16]. Like slip displays, pin arrays also tend to be large and cumbersome. Despite this challenge, Sarakoglou et al. designed a compact 4x4 pin array to be used with an Omega7 kinesthetic feedback device to investigate the benefits of tactile feedback during teleoperation [19]. Their device is compact enough to also be used to evaluate the effects of a pin array in multifinger manipulation.

As an alternative, some devices present the orientation of the contacted surface in order to contribute to shape recognition of virtual objects [2], [20]. Dostmohamed and Hayward present a spherical 5-bar mechanism that is used to orient a 2-DOF tilting plate to match the tangent plane of a virtual surface. The motion of the tilting plate is combined with the user's kinesthetic motions to display curved objects [20]. Frisoli et al. expanded upon this work by miniaturizing the device and adding a mechanism to make and break contact with the user's fingertip [2]. However, the revised device is still too large and cumbersome to be integrated into a multifinger setup.

Chinello et al. developed a similar tactile device using a small tilting plate beneath the fingerpad. Contact force of the plate in different directions is provided by three tendons routed to motors worn on the back of the user's finger [21]. This device was utilized by Prattichizzo et al. in a multifinger pinch needle insertion task [22]. They reported that the tactile feedback provided by their devices could be used in place of kinesthetic feedback with no loss in performance.

Finally, Provancher et al. developed the contact location display, used in previous studies [4], [5], [23]. This device renders the point of contact between the user's finger and a virtual object along the proximal-distal direction of the finger (i.e., a 1-DOF mechanism). The original device was developed for use in planar environments. The device was expanded to 2-DOF with the addition of a second actuator and a spherical 5-bar mechanism by Muhammad et al. [6]. However, numerous problems with the device in addition to its large size prevent it from being used in a multifinger setup.

4.3 Device Design

The concept of contact location feedback is presented in Figure 4.1. Rather than providing all possible tactile information to the user, only the center of contact is rendered through a small contactor. In previous devices, this contactor ("tactor" for short) was only capable of motions in the proximal-distal direction and was actuated through push-pull wires driven by an actuator box mounted on the user's forearm [5], [6] or moved in two-dimensional space over the pad of the finger from a grounded actuator box, but this latter device had a very limited workspace and a large amount of tactor backlash [6].

The new tactile device presented herein (see Figure 4.2) moves the contactor in both proximal-distal and radial-ulnar directions, while also increasing the tactor's range of motion and decreasing the device's size and weight. The compact design of the device

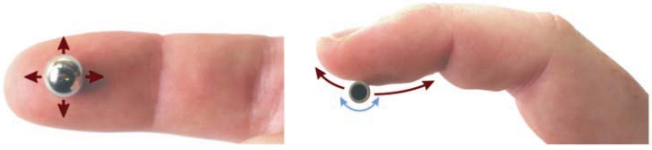

Figure. 4.1 Concept for contact location feedback. The two-dimensional (left) or one-dimensional (right) center of contact is represented with a single tactile element.

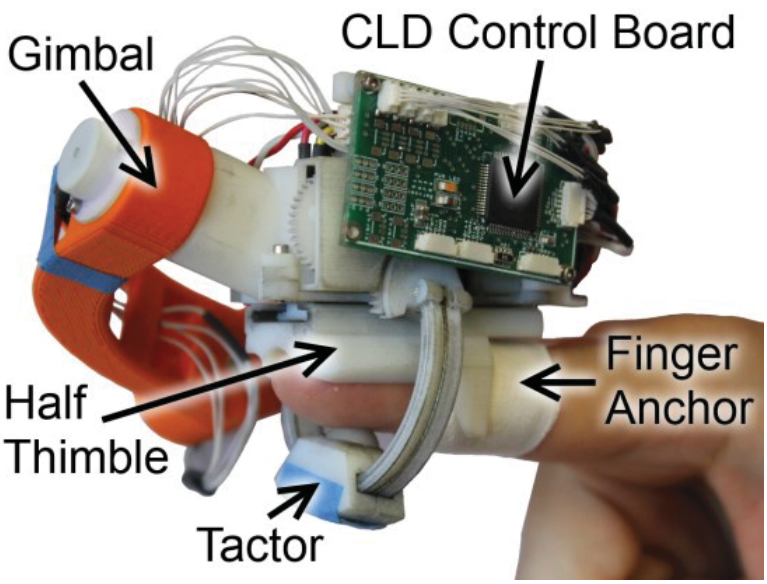

Figure. 4.2 2-DOF contact location display device. The new design moves in both the proximal-distal and radial-ulnar directions.

makes it possible to investigate the effects of providing contact location in multifinger manipulation tasks. The new workspace covers most of the bottom hemisphere of a finger, allowing the device to touch the sides and even the tip of a finger. The contact location display (CLD) device is mounted to a custom kinesthetic feedback device (with capabilities similar to a Phantom Premium 1.5) via a passive three degree-of-freedom gimbal. The gimbal allows full rotational motion of the finger and is capable of sensing orientation through three rotary position sensors (potentiometers).

The 2-DOF CLD is anchored to the user's finger at the medial phalange through a flexible joint. This allows the user's finger to bend naturally when interacting with virtual objects and makes the device more comfortable and natural to use. This increased flexibility also allows the kinesthetic forces applied to the device to be transmitted through the tactor, thus localizing both tactile and kinesthetic feedback to the contact location. When the finger is extended, it rests in a form-fitting half thimble on the bottom

of the device. This half thimble helps minimize any radial-ulnar motions of the finger with respect to the device, keeping it properly aligned. During experiments with only kinesthetic feedback, the CLD is held stationary and the bottom plate is replaced with a full thimble to constrain the finger. Different sized thimbles can be interchanged onto the CLD to accommodate a wide range of finger sizes.

4.3.1 Device Actuation

The 2-DOF CLD is driven by three actuators. These actuators allow the tactor path to match a user's finger profile and give smooth and consistent tactile feedback throughout the device workspace. Figure 4.3 shows the 2-DOF CLD device with each of the three actuation motions highlighted in a different color. Proximal-distal motion of the tactor is achieved by positioning a sliding plate (shown in blue) and a tilting ring (shown in

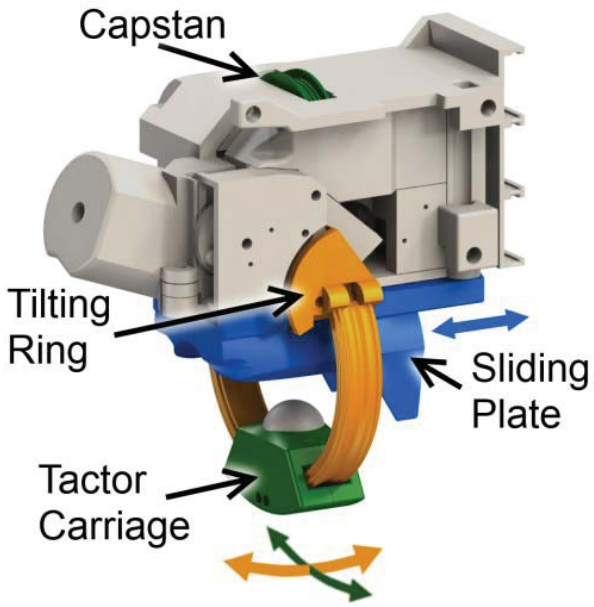

Figure. 4.3 2-DOF CLD device actuated mechanisms. The sliding plate is shown in blue, the tilting ring is shown in orange, and the capstan drive and carriage are shown in green.

orange). Radial-ulnar motion is achieved by the positioning of a carriage around the tilting ring via a capstan pulley design (shown in green).

The sliding plate is driven by a rack and pinion mechanism. The tilting ring hinges on a hollow pin and is directly driven by its gear train. The capstan pulley's cable is made of low-stretch fishing line (Stealth Braid Spiderwire SS50Y-125) and passes through the hollow pin that acts as the hinge of the tilting ring. This is done so that cable length remains constant regardless of ring angle. Both the sliding plate and tilting ring are actuated by the 10 mm motors and gear trains removed from Futaba S3154 servos. The capstan pulley is driven by a 12 mm 100:1 high power micro metal gear motor from Pololu.com (part number: 1101). All three actuators utilize a rotary position sensor (potentiometer) connected to their output to minimize backlash, and are positioned by the integrated control board obtained from Futaba S3154 servos. All housing and actuated components were rapid prototyped by an Eden 260V Objet 3D printer out of Vero White material. Friction between rapid prototyped surfaces was substantially higher than initially expected. This problem was reduced by minimizing contact area on sliding surfaces and using graphite dust to reduce friction. Building the device from materials such as nylon or delrin would substantially reduce the friction between the actuated components and improve the speed and power efficiency of the device.

4.3.2 Device Characterization

The device weighs approximately 45 grams (weight of gimbal not included) when fully assembled. The servo control boards can achieve rotary positions to within 0.0022 radians, which results in 53 μm CLD tactor position resolution. The device has a bandwidth in excess of 5 Hz. The system was characterized with low backlash levels for

all three actuators. The sliding plate contains 510 μm of backlash, the rotary joint contains 0.017 radians of backlash, and the capstan pulley at the tactor contains 420 μm of backlash. Backlash was determined by identifying the smallest amplitude sin wave of commanded positions that still produced noticeable motion at the output under 15x magnification. This translates to a maximum device backlash of 1.13 mm in the proximal-distal directions and 420 μm in the radial-ulnar directions. These values are all less than the reported detectable thresholds given by [23]. The device communicates with a computer via a Microchip dsPIC33E microcontroller using USB communication with no more than 2 ms of delay. Device positions are communicated at 500 Hz.

4.3.3 Advantages and Disadvantages

The primary advantages of this 2-DOF CLD are its larger workspace and lower backlash than the previous 2-DOF CLD device [6]. The device can also be customized to a particular size of finger by replacing the half thimble on the sliding plate and changing the size and position of the ring. Additionally, larger rings can be used to simulate making and breaking contact with the tactor, while smaller rings will cause the tactor to stay in contact with the finger at all times. This gives a sense of presence of an object even when not in contact with the object. A finger profile can be used to drive the tactor smoothly and uniformly across the user's fingerpad. This allows for more comfortable and accurate interactions with virtual objects.

However, the 2-DOF CLD still has a few problems to be worked out in later generations. The largest of these occurs when the ring is too large or the half thimble on the sliding plate is not sized appropriately for the finger. In these cases, it becomes

possible for the finger to be pinched between the tactor and half thimble as the device shifts off center in the radial-ulnar direction (see Figure 4.4). This occurred more often when the device was used in a sideways orientation, due to its center of mass being located away from the finger (see Figure 4.2). To limit this from occurring during experimentation and to allow the device to fit a wide range of finger sizes, the rings were sized at 19 and 21 mm in radius for the devices used with the index finger and thumb, respectively. This placed the tactors lightly in contact with the average participant's fingerpads. Rings sized for smaller fingers could not be used by participants with large fingers and vice versa. Different sliding plates with integral thimbles were provided to match participant finger sizes. Counterbalance weights could also be used to help

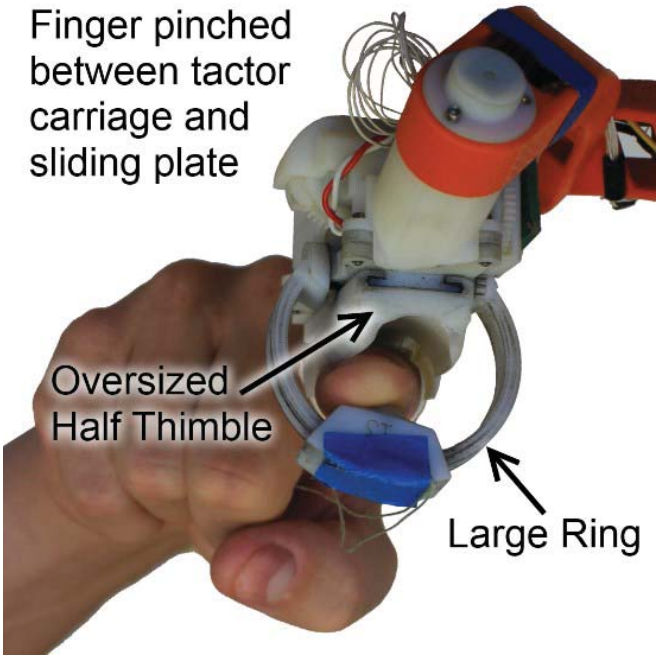

Figure. 4.4 The finger is pinched between the tactor and half thimble on the sliding plate. This occurs when the ring is too large and/or the half thimble is improperly sized. The image shows an index finger being used with a ring and half thimble meant for a thumb.

mitigate the problem, though inertial forces could still cause shifts of the device on the user's finger.

4.4 General Methods

Two separate experiments were conducted to evaluate the new CLD device and to determine the effects of providing contact location on manipulation tasks using two fingers. The experiments evaluate two separate aspects of manipulation: picking up an object and reorientation of an object. Both experiments were performed under two rendering conditions: once with only force feedback, and once with both the CLD and force feedback. The CLD tactor was prepositioned at the closest point of contact when the CLD was within 30 mm of the experiment objects and centered outside of this region, as found to be preferred by users in [6]. In the first experiment, participants were asked to pick up a series of virtual spheres with varying levels of friction. The second experiment required participants to first explore an object, and then orient that object with respect to the monitor in front of them. Each experiment was performed by the same group of twelve participants (2 female, 1 left handed). Participant ages ranged between 19 and 42 with an average age of 28. Nine of the participants had prior experience using the CLD device in previous experiments.

Both experiments were performed in the same session. Half the participants performed both experiments with only force feedback first, then both experiments with both CLD and force feedback. The other half received the opposite order of rendering conditions to provide balanced testing. Between each experiment, participants took a short break to reduce fatigue effects, and then underwent a brief training period to familiarize them with the next experiment's task and rendering condition. Each

experiment took approximately 10-15 minutes to complete, with both pairs of experiments taking approximately 1-1.5 hours in total, including instruction and breaks.

Participants stood for the duration of the experiment. The devices were visually obscured by a board extending to the participant's chest/neck. Experiment instructions were provided on the computer monitor, but no other visual feedback was provided. White noise was played on noise-canceling headphones during testing to mask any auditory cues generated by device motion. Additional audio cues were provided to assist in the pacing of the experiment and to indicate transitions between stimuli. The experimental setup can be seen in Figure 4.5. The experimental setup utilized two CLD devices, each with their own kinesthetic device, attached to the participant's index finger and thumb, respectively. The kinesthetic devices were oriented opposite each other to either side of the hand to provide the largest available workspace. Device gimbals were

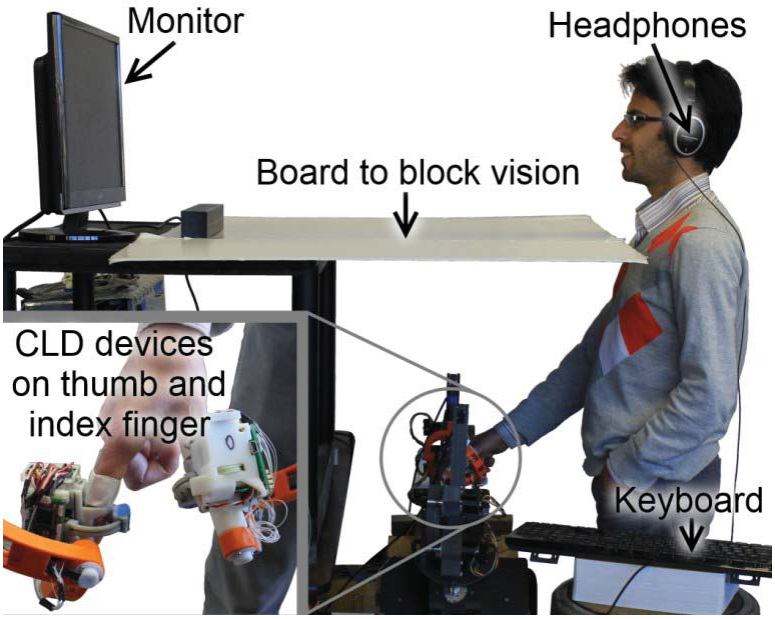

Figure. 4.5 Experiment setup. Participant vision of the device is obscured by a board extending to their chest/neck. White noise is played on noise canceling headphones to eliminate audio cues.

also oriented to minimize potential collisions between a gimbal and the CLD device on the other finger.

4.5 Sphere Pickup Task

The first experiment evaluates a participant's ability to successfully pick up a series of spheres with varying levels of friction. This task is dependent on the ability of the participant to accurately identify the position of the sphere and grasp it with diametrically opposing contact points.

4.5.1 Methods

Participants were instructed to grab the sphere and lift it more than 160 mm above the virtual table. The virtual table's height was adjusted for each participant. This allowed a comfortable grasping posture (as shown in Figure 4.5) and removed any shifting or leaning that could add to fatigue or add to error within the results.

4.5.2 Stimuli

A single sphere of radius 35 mm on a table is rendered to participants during this experiment. Full object dynamics are rendered for the sphere, including gravity and friction. In order to assist in locating the sphere during the experiment, the sphere is held stationary when only one finger is in contact with it. This allows participants to find the sphere again if it slips from their fingers or is dropped. This also gives participants a better sense of the sphere's position to help them align their fingers before grasping. Additionally, the sphere loses all momentum when it is not in contact with the fingers. This stops the sphere from rolling away when it slips or is dropped, and helps participants to find the sphere faster and more reliably. When first placed, the center of the sphere is

shifted up to 15 mm in a random direction along the virtual table's surface. This prevents participants from developing muscle memory for grasping the spheres and giving biased results.

The sphere pickup task was evaluated under three different friction coefficients (0.2, 0.3, and 0.4) between the fingers and the sphere. These friction levels were determined using pilot testing data. Friction levels showed a wide range of success rates, with 0.2 being difficult for most users, and 0.4 being relatively easy but still showing some level of difficulty. Friction coefficients above 0.5 showed almost 100% success rates when picking up the sphere on the first try, while coefficients below 0.1 proved to be nearly impossible to pick up for all but the most skilled participants. The sphere could not be picked up under any of the evaluated friction levels when the participant's fingers were in contact with the table. Thus, while the table could be used to quickly find the sphere, it could not be used to assist in the pickup task.

4.5.3 Procedure

Each of the three tested friction levels was evaluated 30 times, in random order, for a total of 90 trials during the experiment. Each trial consisted of the following sequence. First, the participant moved his/her fingers to a starting configuration. A visual representation of the participant’s fingers and the target zone were shown on the monitor while small pulling forces were applied to the fingers to assist with finger placement. Once the participant’s fingers were in the target zone for 0.5 seconds, the visual indicators were removed and a new sphere was placed below the participant's fingers. The participant would then lower his/her fingers, locate the sphere, and attempt to pick up and raise the sphere 160 mm above the virtual table. If successful, they would proceed to

the next trial. Otherwise, they would continue attempting to pick up that sphere from the new location it slipped to until they had made 5 such attempts. An individual attempt consists of a slip that results in the center of the sphere moving more than 3 mm while the fingers are in contact with the sphere. This is true whether the sphere is on the table or picked up. If the participant felt they had lost track of the sphere and could not find it again, they were allowed to indicate so by pressing a key on the keyboard. Doing so recorded the loss and current number of attempts, and then proceeded to the next trial.

At the end of the entire session, participants were asked which of the two rendering conditions (force-only vs. force + CLD) they believed they performed better in. They were also asked to identify which rendering condition provided a better sense of the sphere's motion during slip and its position relative to their fingers.

4.5.4 Pickup Task Results and Discussion

No effects of testing order or prior experience were observed. Approximately 1% of all trials resulted in a lost sphere. These trials are treated as 5 failed attempts for a trial in the following analysis. Figure 4.6 shows the mean and 95% confidence intervals of the number of failed attempts for the tested friction coefficients and rendering conditions. The mean number of failed attempts for each friction coefficient and rendering condition passes an omnibus ANOVA test [$F(5,2154) = 10.94$, $p < 0.001$]. A post hoc Tukey's test shows a statistically significant improvement in success rates when CLD feedback is provided for the friction coefficients of 0.2 and 0.3. The 0.4 friction coefficient was not shown to be significantly different between the force-only and force + CLD rendering conditions. As friction decreases, the number of failed attempts significantly increases for both the force-only and force + CLD rendering conditions. The improvement shown by

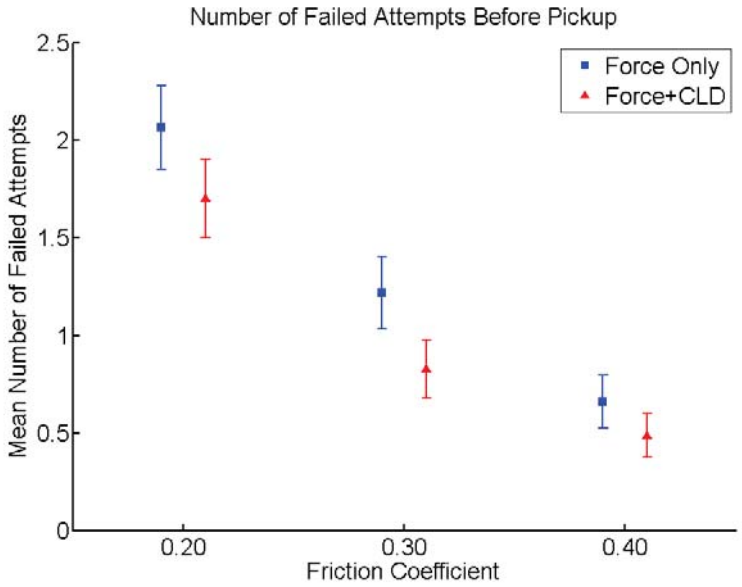

Figure. 4.6 Means and 95% confidence intervals of the number of failed attempts for each friction level under force-only and force + CLD conditions. As friction decreases, the number of failures increases. The addition of CLD significantly decreases the number of attempts, increasing success rates, for friction coefficients of 0.2 and 0.3.

the addition of the CLD matches the reports from the postexperiment survey. In the survey, the majority of participants reported performing better with the CLD and getting a better sense of the sphere's location and motions with the CLD. This improvement is most likely due to the increased sensitivity to surface contours that the CLD provides [5], as well as the radar-like effect that occurs when the tactor remains in contact with the participant's fingerpad while prepositioning [6]. The lack of improvement when using the CLD under a friction coefficient of 0.4 is likely due to the overall ease of the task. The benefits of the CLD are reduced due to a ceiling effect, where participants cannot perform any better regardless of device improvements.

The mean time to completion of the sphere pickup task did not significantly change with rendering conditions [$F(1,2154) = 0.128$, $p = 0.720$]. This indicates that while the CLD did help participants to better grasp the spheres, it did not significantly reduce the

time to find the object or position their fingers. As expected, decreasing friction coefficients caused a significant increase in mean time to completion [$F(2,2157) = 24.74$, $p < 0.001$]. Figure 4.7 shows the mean and 95% confidence intervals of the time to completion under the tested friction coefficients and rendering conditions. The decreased number of failed attempts without any changes in completion time indicates that the CLD provides a benefit when attempting to grasp difficult objects.

4.6 Cylinder Alignment Task

The second experiment evaluates a participant's ability to successfully identify the orientation of an object and to reorient that object with respect to the monitor in front of them. The monitor provided a convenient alignment frame. This task is dependent on the ability of the participant to successfully grasp the object in a known orientation and then reposition it.

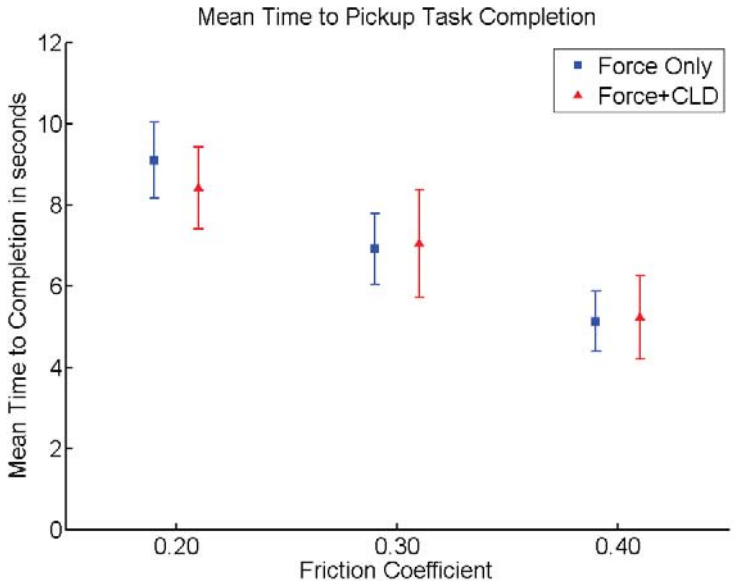

Figure. 4.7 Means and 95% confidence intervals of the time to completion for each friction level under force-only and force + CLD conditions. As friction decreases the time required to complete the task increases. However, the CLD provides no speed benefit to the task.

4.6.1 Methods

Participants were instructed to explore a D-shaped extruded cylindrical object with both fingers and identify the orientation of the flat face. Once identified, they were to pick up and rotate the cylindrical object such that the flat face was parallel with the monitor. The flat face could either be on the near or far side. As in the sphere pickup task, the virtual table's height was adjusted for each participant to allow a comfortable grasping posture (as shown in Figure 4.5) and to remove any shifting or leaning that could add to fatigue or add to error within the results.

4.6.2 Stimuli

A single D-shaped extruded cylindrical object (see Figure 4.8) on a table is rendered to participants during this experiment. The cylindrical object is 35 mm in radius and 70 mm tall. Full object dynamics are rendered for the cylindrical object, including gravity

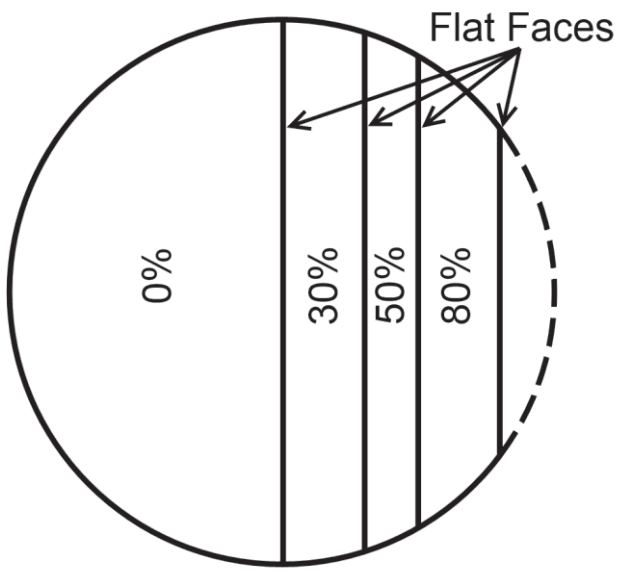

Figure. 4.8 D-shaped extruded cylindrical shape. The shape is made from a cylinder with one side cut off at a percent of the radius from center. 100% results in a full cylinder while a 0% results in a half circle extrude. 30%, 50%, and 80% were the tested shapes.

and friction. During this experiment, the friction coefficient was set to 0.8 to allow participants to easily grip the object. When dropped, the cylindrical object is constrained to rotate toward vertical to prevent the object from tipping over. When first placed, the flat on the cylindrical object is rotated to face a random direction.

During the exploration phase of each trial, the cylindrical object is held fixed and cannot be moved. This allows participants to identify the orientation of the flat face of the object. Pilot testing indicated that if the object was not fixed initially, participants would nudge the object while exploring, causing them to lose track of the flat face, thus significantly increasing trial time and decreasing accuracy. The object was unlocked by pressing a key on the keyboard.

The cylinder alignment task was evaluated with three different sizes of D-shape to determine if the shape of the object influenced the alignment accuracy. These shapes are constructed by taking a cylinder and slicing off the side at a particular percent of the radius from center (see Figure 4.8). 100% results in a full cylinder, while 0% results in a half circle extrude. The three different tested sizes are 30%, 50%, and 80%. Initial pilot testing indicated smaller flats, such as those near 100%, and thinner objects, such as those near 0%, decreased alignment accuracy.

4.6.3 Procedure

Each of the 3 tested shapes was evaluated 30 times in random order during the experiment. Each trial consisted of the following sequence. First, the participant moved his/her fingers to a starting configuration. A visual representation of the participant's fingers and the target zone were shown on the monitor while small pulling forces were applied to the fingers to assist with initial finger placement. Once the participant's fingers

were in the target zone for 0.5 seconds, the visual indicators were removed, and a new cylindrical object was placed below the participant's fingers. The participant would then lower their fingers and explore the cylindrical object, attempting to find the flat face. Once they had identified the orientation of the cylindrical object, the participant would unlock the object through a key on the keyboard, and then pick up and reorient the object such that its flat face was parallel with the monitor in front of them. Once they let go of the object, its orientation was recorded and the next trial would begin.

At the end of the entire session, participants were asked which of the two rendering conditions (force-only vs. force + CLD) they believed they performed better in. They were also asked which rendering condition provided the most useful information for detecting the flat face and its orientation.

4.6.4 Alignment Task Results and Discussion

No effects of testing order or prior experience were observed. Figure 4.9 shows the mean and 95% confidence intervals of the alignment error in radians for the tested shapes and rendering conditions. Figure 4.10 shows the mean and 95% confidence intervals of the trial completion time for the tested shapes and rendering conditions. The CLD showed no statistical effect on the alignment error [$F(1,714) = 0.60$, $p = 0.439$]. However, the CLD had a negative effect on participant time to completion, increasing trial times by approximately 7 seconds [$F(1,714) = 28.82$, $p < 0.001$]. Contrary to the pilot studies, shape showed no significant effect on the alignment error or time [$F(1,714) = 0.10$, $p = 0.910$] [$F(1,714) = 1.736$, $p = 0.177$]. The effects of shape on alignment may not be strong enough to be shown in this study, potentially being masked by the much larger variance in alignment errors. These results agree with participant responses to the two

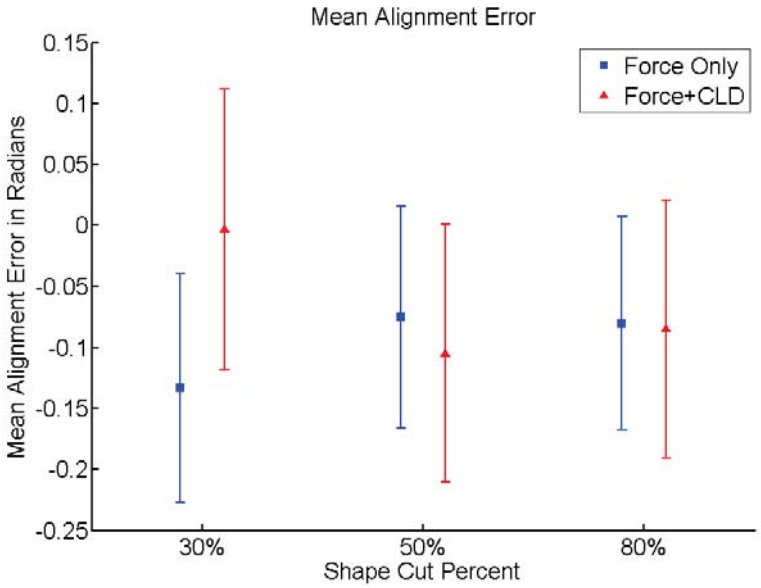

Figure. 4.9 Means and 95% confidence intervals of the alignment error in radians for each tested shape under force-only and force + CLD conditions. Neither shape nor CLD showed any significant effects on the results.

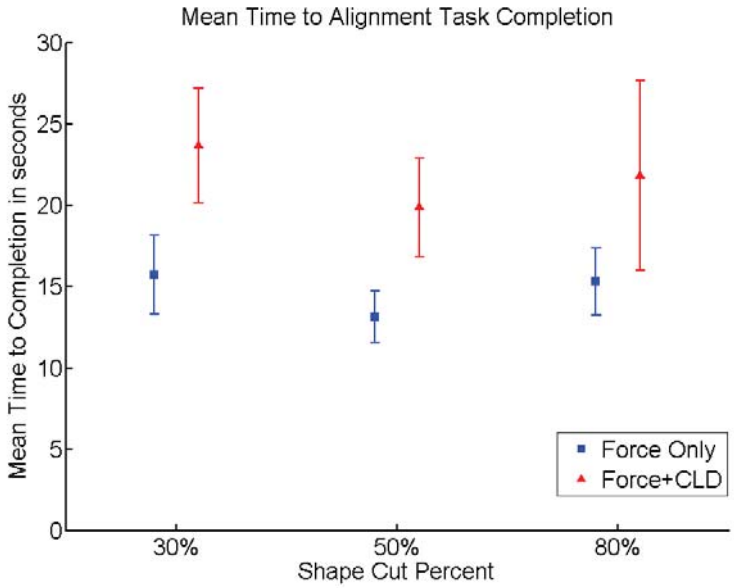

Figure. 4.10 Means and 95% confidence intervals of the time to completion for each tested shape under force-only and force + CLD conditions. CLD feedback significantly slowed participants by an average of 7 seconds.

questions asked at the end of the experiments. The majority of participants responded that they felt the CLD provided redundant information that was not needed to perform the task. Several of them expressed that they found the additional information provided by the CLD distracting, thus causing them to move slower when exploring the shape. These results and responses indicate an oversaturation of information, resulting in a decrease in participant efficiency. This indicates that the CLD should ideally be used in situations where the extra surface information it provides is nonredundant and beneficial to the task. In cases of simple manipulation where this extra information is not helpful, the CLD is not likely to hurt performance, but could potentially slow a user's actions.

When picking up the cylindrical object, participants nearly always positioned one of their fingers near the center of its flat face. Finger alignment errors were evaluated by comparing the angle between the vector formed by the two fingers and the normal of the target plane. Both the alignment error and standard deviation of alignment error are significantly smaller for the finger vector than for the cylindrical object [$t(719) = 2.75$, $p = 0.006$] [$t(719) = -3.39$, $p = 0.001$]. This implies that participants aligned their fingers with respect to the target plane rather than the object. Participants likely assumed they had perfectly grasped the cylindrical object once it was picked up, rather than attempting to sense any irregularities, such as a difference in CLD position and force direction. Alignment errors were minimized when the initial cylindrical object orientation was in an ergonomically comfortable region, i.e., easy to grasp without excessive wrist rotation (see Figure 4.11). The clockwise bias (negative alignment angle) shown in Figures 9 and 11 indicates that participants biased their initial grip counterclockwise. Based on Figure

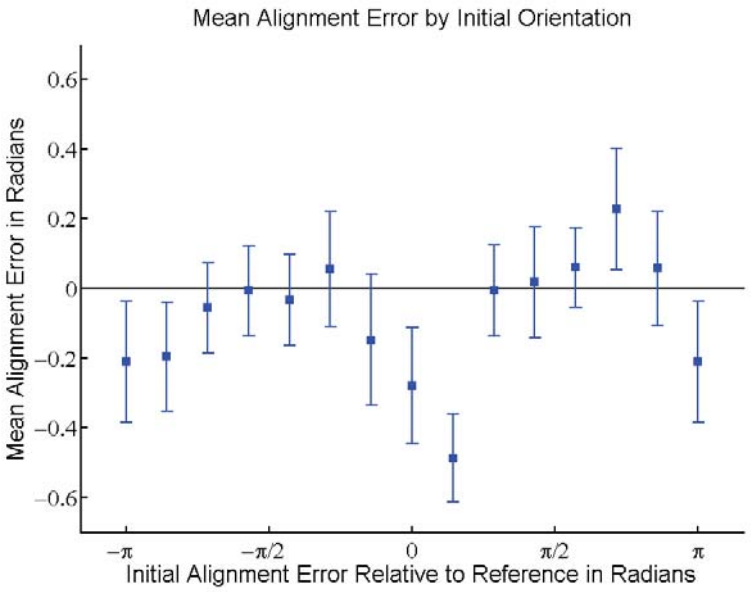

Figure. 4.11 Means and 95% confidence intervals of alignment error as a function of initial object orientation. Force-only and force + CLD results are combined to provide better estimates. Ergonomically comfortable regions show low alignment error while regions that require a large amount of arm twist show larger alignment errors.

4.11, participants would overestimate the angle when gripping outside of a comfortable arm configuration.

4.7 Conclusions and Future Work

A new revision of the CLD device was developed and tested through two simple manipulation experiments. This device is smaller, lighter weight, and contains a larger workspace than its predecessors. The device is capable of full 2-DOF motion along the bottom hemisphere of the finger. It exhibits low backlash and high precision throughout its workspace. The device was shown to meet all the performance requirements in [23] for creating a haptic device without perceivable backlash, lag, or positional inaccuracies.

Two experiments were used to evaluate the device and the effect of providing contact location information during multifinger manipulation tasks. The first experiment evaluated participants' ability to pick up a series of spheres with varying levels of friction.

Participants were able to successfully pick up the spheres in fewer tries when contact location feedback was provided. The addition of contact location feedback did not statistically affect the time it took to pick up the spheres. This showed that the addition of contact location feedback via the CLD device improved participant performance without slowing or hindering the participant. A postexperiment survey showed that participants felt the contact location feedback gave them a better sense of the sphere's position and allowed easier grasping of the sphere. The second experiment required participants to explore a cylindrical object and then orient that object with respect to the monitor in front of them. The addition of contact location feedback was not found to improve participant accuracy, and was shown to increase the time taken to complete the task. The postexperiment survey indicated this time increase was due an oversaturation of haptic information. Participants slowed their exploration to absorb the additional information provided by the CLD, even when it was not needed. Thus, the CLD should ideally be used in situations where the extra surface information it provides is needed for the task. The second experiment also indicated participants would align their fingers, rather than the object, with the monitor. Additionally, participants tended to overcompensate when picking up and reorienting the object when its initial orientation was outside of their ergonomically comfortable wrist orientation.

The revised CLD device was shown to function as expected with a limited number of issues. Before more experiments are run with the device, the flexible joint between the finger and the half-thimble sliding plate should be stiffened in the radial-ulnar direction. This will help to minimize pinching when the half-thimble and ring are inappropriately sized and allow a wider range of finger sizes to be used in future experiments. The design

could also benefit from utilizing different materials as well as strengthening joints and mating surfaces. Future studies will look into how objects are perceived during manipulation and what effects providing additional surface information through the CLD may have.

4.8 Acknowledgments

This work was supported, in part, by the National Science Foundation under awards IIS-0904456 and IIS-0904423.

4.9 References

[1] S. Lederman and R. Klatzky. Sensing and displaying spatially distributed fingertip forces in haptic interfaces for teleoperator and virtual environment systems. Presence: Teleoperators and Virtual Environments, vol. 8, no. 1, pp. 86-103, Feb. 1999.

[2] A. Frisoli, M. Solazzi, F. Salsedo, and M. Bergamasco. A fingertip haptic display for improving curvature discrimination. Presence: Teleoperators and Virtual Environments, vol. 17, no. 6, pp. 550-561, Oct. 2008.

[3] R. Fearing. Tactile Sensing, Perception and Shape Interpretation. PhD thesis, Electrical Engineering: Stanford University, Stanford, CA, USA, 1988.

[4] W. R. Provancher, M. R. Cutkosky, K. J. Kuchenbecker, and G. Niemeyer (2005). Contact location display for haptic perception of curvature and object motion. International Journal of Robotics Research, vol 24(9), pp. 691–702, 2005.

[5] A. J. Doxon, D. E. Johnson, H. Z. Tan, and W. R. Provancher. Force and contact location shading methods for use within two-and three-dimensional polygonal environments. Presence: Teleoperators and Virtual Environments, vol. 20(6), pp. 505-528, 2011.

[6] S. Yazdian, A. J. Doxon, D. E. Johnson, H. Z. Tan, and W. R. Provancher. 2-DOF contact location display for manipulating virtual objects. In 2013 World Haptics Conference (WHC), pp. 443-448, 2013.

[7] A. Frisoli, M. Bergamasco, S. L. Wu, and E. Ruffaldi. Evaluation of Multipoint Contact Interfaces in Haptic Perception of Shapes. In Multi-point interaction with real and Virtual Objects, Springer Berlin Heidelberg, pp. 177-188, 2005.

[8] G. Jansson and L. Monaci. Identification of real objects under conditions similar to those in haptic displays: providing spatially distributed information at the contact areas is more important than increasing the number of areas. Virtual Reality, Vol. 9(4), pp. 243-249, 2006.

[9] H. H. King, R. Donlin, and B. Hannaford. Perceptual thresholds for single vs. Multifinger Haptic interaction. In Haptics Symposium, 2010 IEEE, pp. 95-99, March 2010.

[10] S. McKnight, N. Melder, A. L. Barrow, W. S. Harwin, and J. P. Wann. Perceptual cues for orientation in a two finger haptic grasp task. In Eurohaptics Conference, 2005 and Symposium on Haptic Interfaces for Virtual Environment and Teleoperator Systems, 2005. World Haptics 2005. First Joint, pp. 549-550, March 2005.

[11] Y. Kohno, S. Walairacht, S. Hasegawa, Y. Koike, and M. Sato. Evaluation of two-handed multifinger haptic device SPIDAR-8. ICAT2001, pp. 135-140, 2001.

[12] W. S. Harwin and N. Melder. Improved haptic rendering for multifinger manipulation using friction cone based god-objects. In Proceedings of Eurohaptics conference, pp. 82-85, 2002.

[13] N. Melder and W. S. Harwin. Extending the friction cone algorithm for arbitrary polygon based haptic objects. In Haptic Interfaces for Virtual Environment and Teleoperator Systems, 2004. HAPTICS'04. Proceedings. 12th International Symposium on, pp. 234-241, March 2004.

[14] M. A. Otaduy and M. C. Lin. Stable and responsive six-degree-of-freedom haptic manipulation using implicit integration. In Eurohaptics Conference, 2005 and Symposium on Haptic Interfaces for Virtual Environment and Teleoperator Systems, 2005. World Haptics 2005. First Joint, pp. 247-256, March 2005.

[15] M. Salada, J. Colgate, P. Vishton, and E. Frankel. An experiment on tracking surface features with the sensation of slip. WHC 2005. First Joint EuroHaptics Conference and Symposium on Haptic Interfaces for Virtual Environment and Teleoperator Systems, 2005, pp. 132-137, 2005.

[16] M. Fritschi, M. Ernst, and M. Buss. Integration of kinesthetic and tactile display – a modular design concept. In 2006 EuroHaptics Conference, 2006.

[17] R. J. Webster III, T. E. Murphy, L. N. Verner, and A. M. Okamura. A novel two-dimensional tactile slip display: design, kinematics and perceptual experiments. In ACM Transactions on Applied Perception (TAP), vol. 2(2), pp. 150-165, 2005.

[18] K. Drewing, M. Fritschi, R. Zopf, M. O. Ernst, and M. Buss. First evaluation of a novel tactile display exerting shear force via lateral displacement. In ACM Transactions on Applied Perception (TAP), vol. 2(2), pp. 118-131, 2005.

[19] I. Sarakoglou, N. Garcia-Hernandez, N. Tsagarakis, and D. Caldwell. A high performance tactile feedback display and its integration in teleoperation. IEEE Transactions on Haptics, vol. 5, no. 3. pp. 252-263, 2012.

[20] H. Dostmohamed and V. Hayward. Trajectory of contact region on the fingerpad gives the illusion of haptic shape. Experimental Brain Research, vol. 164, no. 3, pp. 387-94, July, 2005.

[21] F. Chinello, M. Malvezzi, C. Pacchierotti, and D. Prattichizzo. A three DoFs wearable tactile display for exploration and manipulation of virtual objects. In Proceedings of IEEE, Haptics Symposium (HAPTICS), pp. 71-76, 2012.

[22] D. Prattichizzo, C. Pacchierotti, and G. Rosati. Cutaneous force feedback as a sensory subtraction technique in haptics. IEEE Transactions on Haptics, vol. 5, no. 4, pp. 289-300, 2012.

[23] A. J. Doxon, D. E. Johnson, H. Z. Tan, and W. R. Provancher. Human Detection and Discrimination of Tactile Repeatability, Mechanical Backlash, and Temporal Delay in a Combined Tactile-Kinesthetic Haptic Display System. In IEEE Transactions on Haptics, Vol.6(4), pp. 453-463, 2013.

CHAPTER 5

CONCLUSION

This document presented several studies that improve the state-of-the-art in tactile-kinesthetic displays. The first study presented two algorithms for smooth interaction with general polygonal models. These algorithms allow many tactile devices, which generally utilize specialized environments to create smooth interactions, to be used with general polygonal models. They specifically address the rendering issues presented by faceted models when using a tactile display that stop traditional shading algorithms from being used. Two experiments were run to validate these algorithms. The first experiment evaluated the maximum angle between faceted faces for rendering polygonal models as smooth surfaces. The addition of tactile feedback from the CLD significantly increased the ability of participants to detect an edge from a 0.5° to 0.2° angle difference between adjacent polygons. Traditional force shading algorithms only weakly masked the edges when CLD feedback was provided, increasing the angle to approximately 0.22°. The inclusion of the new shading algorithms substantially decreased this perception threshold, allowing the angle between adjacent polygons to increase to ~3.5°. These algorithms allow less complex models, and thus less computational overhead, to be used without compromising the smoothness of the haptic sensation. The second experiment evaluated the CLD device's capability to facilitate dexterous exploration and shape recognition. This experiment demonstrated the efficiency of our 3D algorithm, but pointed out design

flaws in the current CLD device restricting interactions with 3D objects and limiting the usefulness of CLD feedback. Participants were capable of spending nearly twice as much of their exploration time in contact with the object when CLD feedback was provided. However, no other effects of CLD feedback on exploration or identification were shown. This experiment underscored the need for a device revision before running any further experiments using 3D environments.

The second study established previously undefined design criteria for tactile devices by evaluating perception thresholds for cue localization, backlash, and device delay. By designing devices with capabilities similar to these criteria, tactile devices can become smaller, less expensive, and more useful. The results of this study were directly used to improve and expand the CLD design in the third article (Chapter 4). The study found that participants were able to localize tactile cues to within 1.3 mm on their fingerpad. Cue localization was also biased toward the center of the fingerpad. These results stipulate the maximum positioning error the device should achieve after large or sequential motions. Tactor backlash could be detected when larger than 1.16 mm on high curvature surfaces, and 0.69 mm on low curvature surfaces. Curvature significantly affects perception of backlash by changing the relative finger motion necessary to create a specific tactor displacement. In contrast to localization, these thresholds indicate the tactor positioning requirements for small or immediate motions. System delay on tactile output can be as large as 61 ms before being detected. The back-end delay (tactile motion after user motion has ceased) was the dominant cue in detecting system delay. Front-end delay is masked by finger motion and becomes detectable above 132 ms.

The design criteria evaluated in the second study (Chapter 3) was used to design the revision of the CLD presented in Chapter 4. The device meets all these performance requirements for creating a haptic device without perceivable backlash, lag, or positional inaccuracies. The design overcomes many of the deficiencies in the original CLD device presented in Chapter 2 by providing a larger, 2-DOF workspace with low backlash and high precision, while also miniaturizing the device and reducing its weight. The extra degree-of-freedom and larger workspace make the device more useful in 3D environments, while the smaller form factor and lighter weight of this design expand its use to multifinger manipulation and object perception studies.

Two studies into the effects of CLD in multifinger manipulation were used in evaluation of the new device. The first experiment evaluated participant's ability to pick up spheres under different levels of friction. The addition of tactile feedback significantly reduced the number of attempts to successfully pick up each sphere but did not affect completion time. A postexperiment survey showed that participants felt the contact location feedback gave them a better sense of the sphere's position, which allowed easier grasping of the sphere. The second experiment required participants to explore a cylindrical object and then orient that object with respect to the monitor in front of them. The addition of contact location feedback was not found to improve participant accuracy, and was shown to increase the time taken to complete the task. The postexperiment survey indicated this time increase was due an oversaturation of haptic information. Participants slowed their exploration to absorb the additional information provided by the CLD, even when it was not needed. Thus, tactile feedback should ideally be used in situations where the extra surface information it provides is necessary.

These experiments demonstrated the revised CLD device performs well not only in 3D environments but also in multifinger manipulation, expanding not only the usable experiment environments but also providing new avenues of research. The experiments indicated only a few minor issues with the design, all of which are currently being addressed.

5.1 Future Work

The revised 2-DOF CLD, presented in Chapter 4, opened new avenues of research. Most importantly, this design can be used in multifinger systems to evaluate the effects of tactile feedback in grasping and manipulation experiments. This allows experiments evaluating how people perceive and manipulate grasped objects, as well as how their perception can be altered through alternate feedback from the CLD device. There are very few studies investigating the perception of grasped objects, making this a novel and interesting direction of research. Further experiments would identify the difference in performance between the prior 1-DOF CLD device and the new 2-DOF CLD device, specifically addressing the differences created by including the additional DOF. Throughout all future work, the CLD device and its control will continue to be refined and improved.